

## 22. PALEOMAGNETISM OF IGNEOUS ROCKS DRILLED ON LEG 114<sup>1</sup>

E. A. Hailwood<sup>2</sup> and N. Vashisht<sup>2</sup>

### ABSTRACT

A paleomagnetic study was made of 12 samples of trachytic basalt from the base of ODP Hole 698A on the Northeast Georgia Rise (southwest Atlantic) and four samples of andesitic basalt and nine samples of volcanic breccia from the base of ODP Hole 703A on the Meteor Rise (southeast Atlantic). The magnetic intensities of the Hole 703A samples are anomalously low, possibly reflecting alteration effects. The mean magnetic intensity of the Hole 698A samples is high, and compatible with the model of Bleil and Petersen (1983) for the variation of magnetic intensity with age in oceanic basalts, involving progressive low-temperature oxidation of titanomagnetite to titanomaghemite for some 20 m.y. followed by inversion to intergrowths of magnetite and other Fe-Ti oxides during the subsequent 100 m.y. These results support the interpretation of the Hole 698A basalts as true oceanic basement of Late Cretaceous age rather than a younger intrusion.

Well-defined stable components of magnetization were identified from AF and thermal demagnetization of the Hole 698A basalts, and less well-defined components were identified for the Hole 703A samples. Studies of the magnetic homogeneity of the Hole 698A basalts, involving harmonic analysis of the spinner magnetometer output, indicate the presence of an unevenly distributed low-coercivity component superimposed on the more homogeneous high-coercivity characteristic magnetization. The former component is believed to reside in irregularly distributed multidomain magnetite grains formed along cracks within the basalt, whilst the latter resides in more uniformly distributed finer magnetic grains.

The inclination values for the high-coercivity magnetization of five Hole 698A basalt samples form an internally consistent set with a mean value of  $59^\circ \pm 5^\circ$ . The corresponding Late Cretaceous paleolatitude of  $40^\circ \pm 5^\circ$  is shallower than expected for this site but is broadly compatible with models for the opening of the South Atlantic involving pivoting of South America away from Africa since the Early Cretaceous.

The polarity of the stable characteristic magnetization of the Site 698 basalts is normal. This is consistent with their emplacement during the long Campanian to Maestrichtian normal polarity Chron C33N.

### INTRODUCTION

During Ocean Drilling Program (ODP) Leg 114 a set of seven sites was drilled in a transect across the southern South Atlantic at a latitude of about  $50^\circ\text{S}$ . This transect extends from the Northeast Georgia Rise in the west to the Meteor Rise in the east (Fig. 1). The main purpose of the drilling was to investigate the late Mesozoic and Cenozoic paleoceanographic and subsidence history of this region, documented in the sedimentary record.

Drilling terminated in igneous rocks, thought to form part of, or to be closely related to, volcanic basement at three of the sites (698, 701, and 703). At Site 701, the recovery of igneous rocks consists of a single 8-cm-long piece of amygdaloidal olivine basalt, from the bottom of the hole in Core 114-701C-52W at a depth of 481 m below seafloor (mbsf). The overlying sediments are early middle Eocene in age. At Site 698 a ~10-m-thick sequence of sparsely phyrlic, holocrystalline, trachytic and subtrachytic basalts in Cores 114-698A-24R and 114-698A-25R and the upper 28 cm of Core 114-698A-26R overlies a hematitic claystone unit, at least 80 cm in thickness, in Core 114-698A-26R and a weathered basaltic regolith in Core 114-698A-27R. The sediments overlying the basalt are Late Cretaceous in age. At Site 703 a volcanic breccia comprising partly-cemented pumice and volcanic glass shards was recovered in Core 114-703A-34X. Recovery in the underlying Cores 114-703A-35X to 114-703A-39X was

almost zero, but in Core 114-703A-40X a dolomite-bearing volcanic ash-calcareous sand unit, believed to represent a mass-flow deposit, overlies 1.65 m of slightly altered porphyritic/andesitic basalt, which occurs as pieces intermixed with volcanic carbonate sand in Core 114-703A-40X and as fragments retrieved in the core catcher of Core 114-703A-41X. The sediments overlying the volcanic breccia are early middle Eocene in age.

Because of the very limited recovery of igneous rocks at all three sites it is not certain whether these rocks represent true basement or igneous intrusions associated with the basal sediments. However, the seismic profiles at all three sites indicate that drilling probably terminated either at or very close to true basement.

The thickness of igneous rock recovered at Site 701 (8 cm) was insufficient to justify paleomagnetic investigations, but sufficient material was available from Sites 698 and 703 for limited paleomagnetic studies to be carried out. The main purpose of these studies is to define the direction of characteristic remanent magnetization in these rocks, in order to establish its possible contribution to observed marine magnetic anomalies and to provide preliminary information on the possible paleolatitude of these sites at the time of initiation of sedimentation. This will contribute to models of the tectonic evolution of the region. A subsidiary aim is to obtain information on the homogeneity of magnetization in oceanic igneous rocks.

### ROCK SAMPLES

All of the samples were taken aboard ship by either cutting 10-cm<sup>3</sup> cubes or drilling 2.5-cm-diameter core plugs from the working halves of the cores. The lengths of the core plugs

<sup>1</sup> Ciesielski, P. F., Kristoffersen, Y., et al., 1991. *Proc. ODP, Sci. Results, 114*: College Station, TX (Ocean Drilling Program).

<sup>2</sup> Oceanography Department, Southampton University, Southampton SO9 5NH, UK.

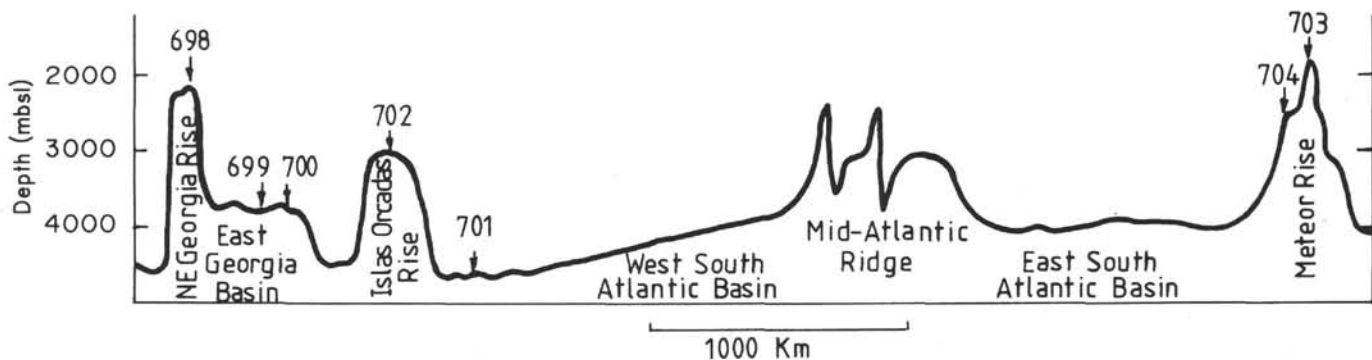


Figure 1. Schematic profile across the southern South Atlantic at a latitude of approximately 50°S, showing the location of the ODP Leg 114 drill sites.

were typically 3 to 4 cm, so it was possible to cut either one or two cylindrical samples, 1.5 to 2.5 cm in length, from each plug for the paleomagnetic analyses. Where two samples were cut, that closest to the axis of the core was labeled *A* and the other *B*. Each sample was cut from a separate rock piece. Because of the azimuthal randomization of the pieces caused by rotary drilling, the reference azimuth for each piece (perpendicular to the split-core surface) is different.

A total of eight samples was taken from the basalts of Hole 698A. Two samples each were cut from four of the original Hole 698A samples and a single sample from each of the others, providing a total of 12 samples from this hole. For Hole 703A a total of nine samples was cut from seven plugs drilled in pieces of volcanic breccia from Core 114-703A-34X and four samples from three plugs in the andesitic basalts of Core 114-703A-40X. Relevant details of the samples are listed in Table 1.

### PALEOMAGNETIC INVESTIGATIONS

All remanence measurements in this study were carried out using a Molspin balanced fluxgate spinner magnetometer. This instrument operates by rotating the rock sample about a vertical axis at a rate of 7 Hz, within a fluxgate ring sensor. The output from this sensor is digitized and stored in a microcomputer so that the signal can be integrated over a specified number of revolutions, in order to build up the signal at the expense of random magnetic noise within the sensing region. The two components of magnetization within the plane of rotation are derived from a Fourier analysis of the waveform generated by this rotation. By spinning the sample consecutively about three orthogonal axes (in the "upright" and "inverted" position, giving a total of six spins) each of the three Cartesian components of remanence is determined four times. The average of these four determinations is then used to calculate the vector resultant.

In its standard form this magnetometer uses only the first harmonic of the waveform, with the higher harmonics not determined. If the magnetization is completely homogeneous (or if the ferromagnetic mineral grains carrying this magnetization are homogeneously distributed within the sample) then this magnetization is effectively represented by a dipole at the geometric center of the sample and is completely specified by the first harmonic. However, if the magnetization is unevenly distributed the higher harmonics will become significant and, in principle, a determination of these higher harmonics should allow a specification of the degree of inhomogeneity. Information on the degree and nature of magnetic inhomogeneity in rock samples on a centimeter scale is virtually nonexistent, yet such information may well assist in understanding the history and processes of magnetization in rocks. For this

reason it was decided to attempt magnetic homogeneity determinations on the Leg 114 igneous rock samples.

There is no record in the literature of this type of analysis using a balanced fluxgate spinner magnetometer. To achieve the analysis the standard magnetometer was fitted with a modified processor, which allowed the output from the fluxgate ring sensor to be sampled by an external computer, rather than analyzed by the internal microprocessor. The computer used for this analysis was a BBC "Master," which was also used to control the operation of the magnetometer. The raw signal was stacked within the computer for a set number of revolutions and the stacked waveform could be viewed on the screen of a visual display unit to monitor the effectiveness of the signal integration and noise rejection at any stage. When a satisfactory level of signal integration had been achieved (normally 32 revolutions for these high-intensity rocks) a listing of the first 10 harmonics was produced from Fourier analysis of the waveform. The resultant magnetization was calculated from the first harmonic in the standard way, but the availability of data on the relative amplitude of the higher harmonics allows an assessment to be made of the degree of inhomogeneity. For the purposes of this preliminary study this was achieved by a simple analysis of the ratio of the second to the first harmonic (because the amplitude of the second harmonic was almost invariably greater than that of all other higher harmonics).

A representative subset of 14 samples from the two holes was subjected to incremental alternating field (AF) demagnetization at peak fields up to 30 mT using a Highmoor AF demagnetizer with a two-axis tumbler. Magnetic homogeneity analyses were carried out for the remanence measured after each demagnetizing step for three samples from Hole 698A, with the specific aim of establishing whether the distribution of low-coercivity components differs from that of high-coercivity components within these samples. A further subset of 11 samples was subjected to incremental thermal demagnetization, using a Schonstedt SM-1 thermal demagnetizer.

In addition to incremental demagnetization analysis, the bulk magnetic susceptibility and susceptibility anisotropy of one sample from each of the Hole 698A samples was measured using a Highmoor susceptibility bridge and a low-field torque magnetometer, respectively. The torque magnetometer used an applied field of 10 mT at a frequency of 50 Hz. A representative subset of five samples from the two holes was subjected to isothermal remanent magnetization (IRM) acquisition to investigate the nature of the ferromagnetic constituents. The type of experimental work carried out on each sample is summarized in Table 1.

Certain rocks that contain a high proportion of low-coercivity grains acquire a spurious remanent magnetization when

Table 1. Summary of sample analyses, Leg 114.

Reference code	Core, section, interval (cm)	Depth (mbsf)	Core piece length (mm)	Rock type	AF demagnetization	Thermal demagnetization	Magnetic anisotropy	IRM	Inhomogeneity
	114-698A-								
1	24R-1, 130(A)	210.80	95	Trachytic basalt	*		*		*
2	24R-1, 130(B)	210.80	95	Trachytic basalt		*			*
3	24R-2, 81	211.81	109	Trachytic basalt	*		*	*	
4	25R-1, 18	213.68	47	Trachytic basalt		*	*		
5	25R-1, 75(A)	214.25	58	Trachytic basalt	*		*		*
6	25R-1, 75(B)	214.25	58	Trachytic basalt		*			*
7	25R-2, 39	215.39	95	Trachytic basalt		*	*		
8	25R-2, 123(A)	216.23	84	Trachytic basalt	*	*	*	*	*
9	25R-2, 123(B)	216.23	84	Trachytic basalt		*			*
10	25R-3, 41	216.91	80	Trachytic basalt		*	*		
11	25R-3, 124(A)	217.74	102	Trachytic basalt	*		*		
12	25R-3, 124(B)	217.74	102	Trachytic basalt		*			
	114-703A-								
	34X-2, 119	307.59	43	Volcanic breccia	*		*	*	
	34X-3, 31	308.21	76	Volcanic breccia	*		*		
	34X-3, 101(A)	308.91	60	Volcanic breccia	*		*		
	34X-3, 101(B)	308.91	60	Volcanic breccia		*			
	34X-4, 60(A)	310.00	42	Volcanic breccia	*		*		
	34X-4, 60(B)	310.00	42	Volcanic breccia		*			
	34X-4, 99	310.39	50	Volcanic breccia	*		*		
	34X-5, 12	311.02	85	Volcanic breccia		*	*		
	34X-5, 42	311.32	106	Volcanic breccia	*		*	*	
	40X-2, 61(A)	364.01	76	Andesitic basalt	*		*		
	40X-2, 61(B)	364.01	76	Andesitic basalt		*			
	40X-2, 108	364.48	120	Andesitic basalt	*		*	*	
	40X-3, 92	365.82	89	Andesitic basalt	*		*		

rotated during AF demagnetization (e.g., Wilson and Lomax, 1972; Stephenson, 1976, 1980, 1981). Such rotational remanent magnetization (RRM) is generally quite repeatable and can be effectively eliminated by adopting a double-demagnetization procedure in which the sample is demagnetized twice at each applied field value and the direction of rotation is reversed between the two treatments (Hillhouse, 1977). Measurement of the resultant magnetization vector after both stages allows the magnitude of the spurious RRM to be identified by vector subtraction, from which it can be cancelled by vector addition to isolate the natural remanent magnetization (NRM). RRM generally become apparent at high treatment levels, and in the present study the double demagnetization procedure was carried out routinely for all treatments at and above 15 mT. The magnitude of the RRM acquired by a sample provides a measurement of its magnetic stability (low-stability grains are more prone to RRM acquisi-

tion). In general, RRM ratios (RRM/NRM) are small for the Hole 698A samples (~5% or less), whereas values for the Hole 703A samples are significantly greater (commonly 30% to 90%).

#### PALEOMAGNETIC DIRECTIONAL PROPERTIES OF HOLE 698A BASALT SAMPLES

##### AF Demagnetization

The response to incremental AF demagnetization of five basalt samples from Hole 698A is shown on vector end-point plots in Figure 2 (for an explanation of these, see Dunlop, 1979). In these plots the tip of the vector after each demagnetization step is plotted on a pair of orthogonal planes, one horizontal and the other vertical, with a common axis that is "N-S" in these examples. (Because the azimuthal orientation of the core pieces is unknown, N refers to the arbitrary

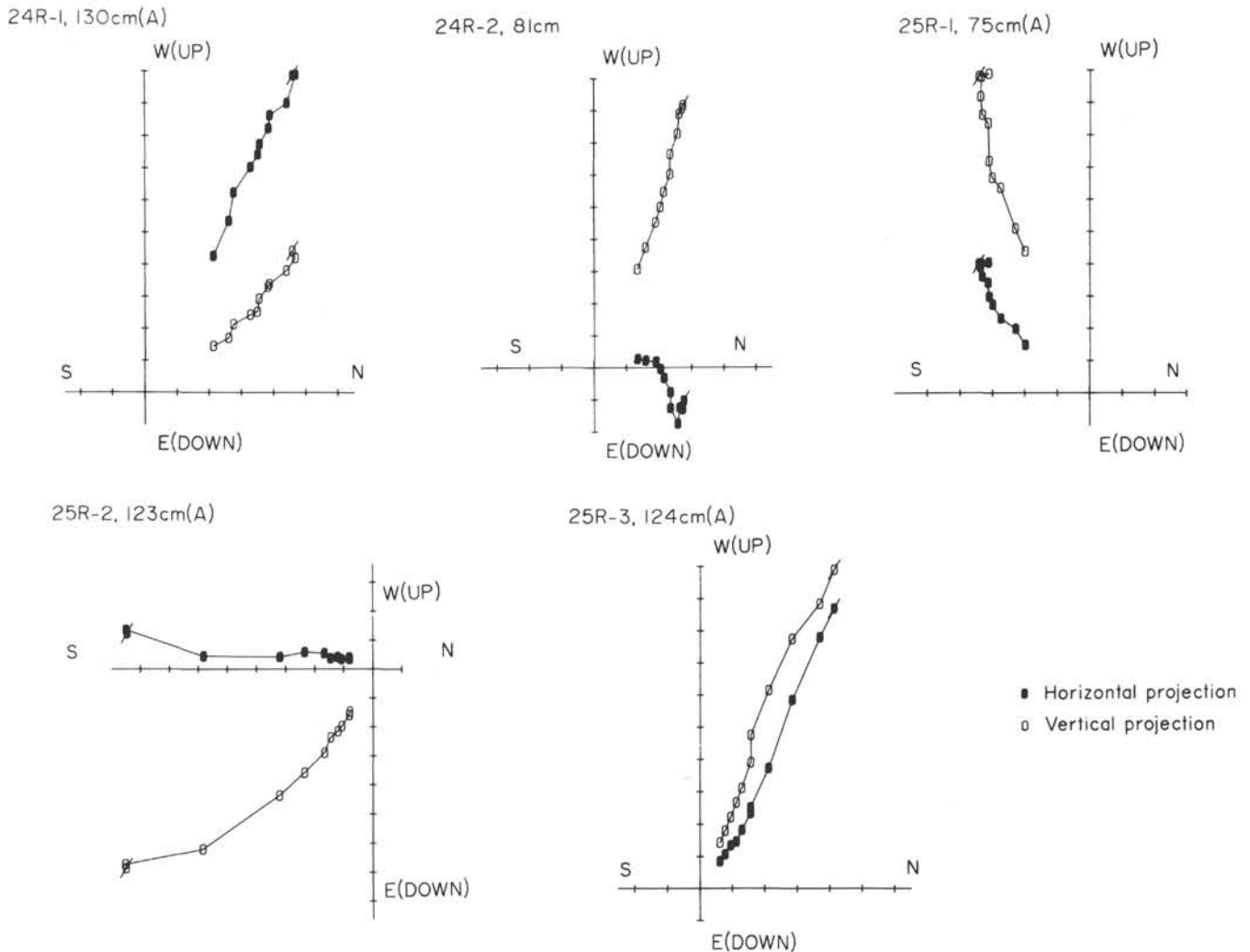


Figure 2. Response of Hole 698A samples to AF demagnetization. The directions of the NRM vectors and the vectors after each demagnetization step are plotted on vector end-point diagrams (Dunlop, 1979). Because the azimuthal orientation of the core pieces is unknown, "N" refers to the arbitrary fiducial direction perpendicular to the split-core face. Corresponding stereographic projection and intensity decay plots are shown in Figure 7. Symbols crossed with a slash represent initial vectors. Demagnetizing field values are 2.5, 5, 7.5, 10, 15, 20, 25, 30, and 35 mT.

fiducial direction normal to the split-core face.) In all five cases small low-coercivity components are removed during the early stages of AF demagnetization (indicated by changes in slope of the lines) but, with the exception of the horizontal component of Sample 114-698A-24R-2, 81 cm, points representing the last few demagnetization steps lie on lines directed through the origin. The directions of the high-coercivity components of magnetization defined from linear regression of these points are plotted in Figure 3A.

As expected from the random azimuthal orientation of these core pieces, there is a wide spread of declination values between samples. Four of the five inclination values lie close to the steep value expected for this high-latitude site (axial geocentric dipole inclination =  $68^\circ$ ). The magnetic polarity of the high-coercivity component of all samples except Sample 114-698A-25R-2, 123 cm (A) (code 8; Fig. 3A), is normal (negative inclination).

#### Thermal Demagnetization

To further investigate the stability of the Hole 698A basalt remanent magnetization, seven additional samples were subjected to incremental thermal demagnetization at temperatures up to  $675^\circ\text{C}$  (Fig. 4). Sample 114-698A-25R-2, 123 cm

(A), the only sample carrying a reverse polarity high-coercivity remanence, was also subjected to this treatment.

In the majority of the samples directional changes were erratic during treatment up to about  $300^\circ\text{C}$ , as viscous components were removed, but thereafter more systematic changes occurred. For clarity the data for treatment up to  $300^\circ\text{C}$  are omitted from most of the plots in Figure 4. Also, the last few steps are shown on an expanded scale in accompanying plots. In all cases random directional changes occurred at and above the  $675^\circ\text{C}$  heating step (the Curie temperature of hematite); thus, these points are not plotted.

For most samples three separate components of magnetization, with different blocking temperature ( $T_B$ ) spectra, have been defined from linear segments on the vector plots (Table 2). The low  $T_B$  component is generally specified by treatment in the range  $300^\circ\text{--}500^\circ\text{C}$ ; the moderate  $T_B$  component at somewhat higher temperatures, up to the Curie point of magnetite ( $575^\circ\text{C}$ ); and the high  $T_B$  component at temperatures between the Curie points of magnetite and hematite ( $575^\circ$  and  $675^\circ\text{C}$ ). In several samples (e.g., Samples 114-698A-25R-1, 75 cm (B), and 114-698A-25R-3, 124 cm (B)), all three components have similar directions, and in the majority of cases the moderate and high components are clearly similar. Thus, the

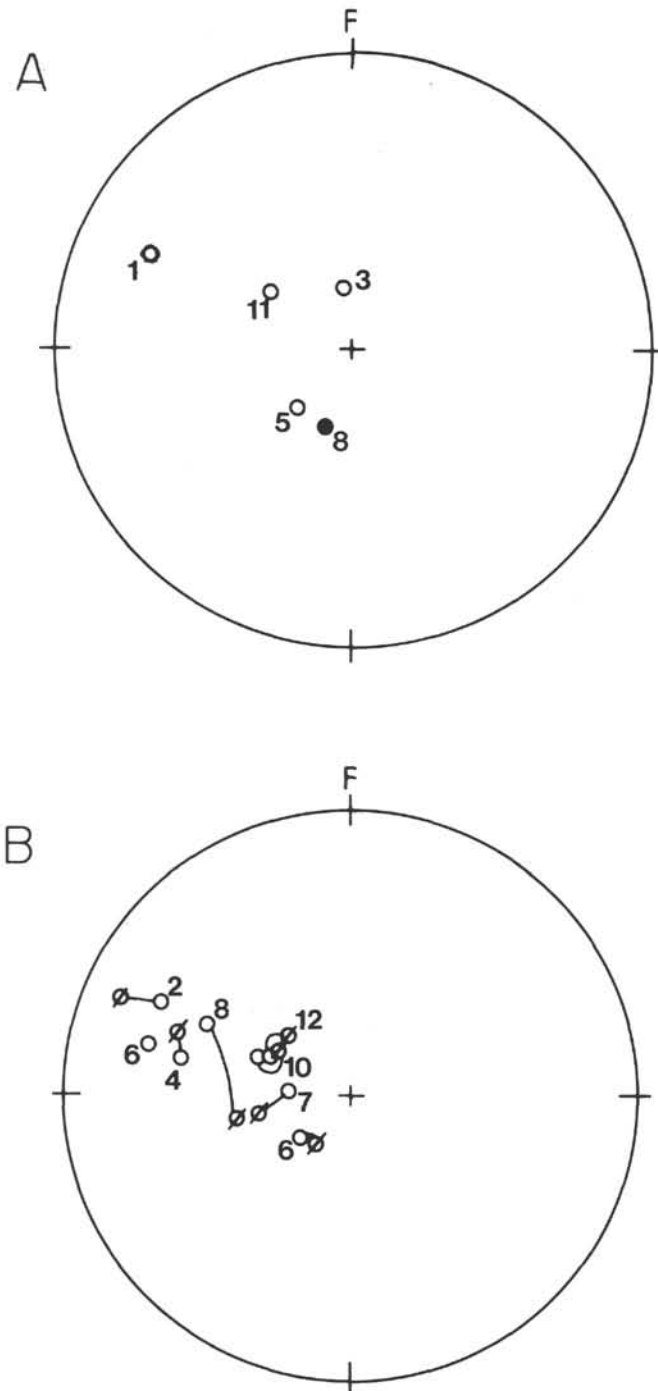


Figure 3. Directions of high-coercivity vectors identified from AF demagnetization (A) and moderate and high blocking temperature ( $T_B$ ) vectors from thermal demagnetization (B) of basalt samples from Hole 698A, shown on stereographic projections. Open circles, upper hemisphere (negative inclination); solid circles, lower hemisphere (positive inclination). Numbers refer to sample codes listed in Table 1. High- $T_B$  vectors are crossed with a slash to differentiate them from moderate- $T_B$  vectors in Figure 3B; vectors from the same sample are linked.

magnetizations carried by the magnetite and hematite grains appear to be closely related.

The reverse polarity component of stable magnetization of Sample 114-698A-25R-2, 123 cm (A), which had resisted AF demagnetization up to 30 mT (Fig. 2) was removed by thermal treatment at 500°C (Fig. 4) to reveal a normal polarity high- $T_B$  component. The sister Sample 114-698A-25R-2, 123 cm (B), from the same core plug, showed similar behavior, but poor repeatability of measurements prevented demagnetization of this sample above 550°C (Fig. 4).

The directions of the moderate and high components defined by thermal demagnetization of the Hole 698A samples are plotted in Figure 3B. These components are closely similar to the high-coercivity component in the core plugs from which samples were subjected to both types of treatment: Samples 114-698A-24R-1, 130 cm, and 114-698A-25R-1, 75 cm.

Despite the arbitrary orientation of the fiducial lines in different samples the moderate and high components show a distinct clustering around a "westerly" azimuth. There is no obvious explanation for this effect, other than a chance similarity in the arbitrary fiducial directions of the samples. (The westerly azimuth does not correspond with the cylindrical axis of the samples, so it cannot be attributed to a drilling-induced remanence).

#### Inhomogeneity of Magnetization

As discussed in the "Paleomagnetic Investigations" section, an attempt was made in this study to explore the degree of homogeneity of the distribution of magnetic mineral grains within the Hole 698A basalts through a Fourier analysis of the magnetometer output. Plots of the relative amplitudes of the first 10 harmonics (expressed as a percentage of the first harmonic amplitude) determined from the NRM measurements on two typical samples are shown in Figure 5. Plots are shown for each of the six spin orientations.

As shown in Table 3, the same pairs of components are measured on spins 1 and 3 (y and z), 2 and 4 (x and z), and 5 and 6 (x and y). For this reason it is expected that the harmonic amplitudes will be similar for each of these pairs of spins (although the phases will be different). Clearly this is the case in Figure 5. The second harmonic was consistently found to be the greatest of the higher harmonics (about 3% to 4% of the first harmonic in the two examples shown), whilst the amplitudes of the other harmonics varied in a more complicated manner. Thus, for the purposes of this initial examination of the degree of magnetic inhomogeneity in the Hole 698A basalts it was decided to use the percentage ratio of the second to the first harmonic amplitude ( $J_2/J_1$ ). This parameter is referred to as the "relative second harmonic amplitude" in the following discussion.

The variation of the relative second harmonic amplitude during AF demagnetization of the three basalt samples from Hole 698A is shown in Figure 6. As with the NRM measurements (Fig. 5) there is a general similarity in values of the relative second harmonic amplitude for spins 1 and 3, 2 and 4, and 5 and 6 for all three sets of analyses.

A conspicuous feature of the results for Samples 114-698A-25R-2, 123 cm (A), and 114-698A-25R-3, 124 cm (A), is the large reduction of the relative second harmonic amplitude after the first few demagnetization steps (i.e., after treatment in fields of about 5 to 7.5 mT). The changes in magnetic direction and intensity during this treatment are shown in Figure 7. In both samples there is a significant reduction of intensity (by 30%–40%) and a steepening of the inclination during the first two to three demagnetizing steps, as a low-coercivity remanence component is removed. The accompanying reduction of the relative second harmonic amplitude

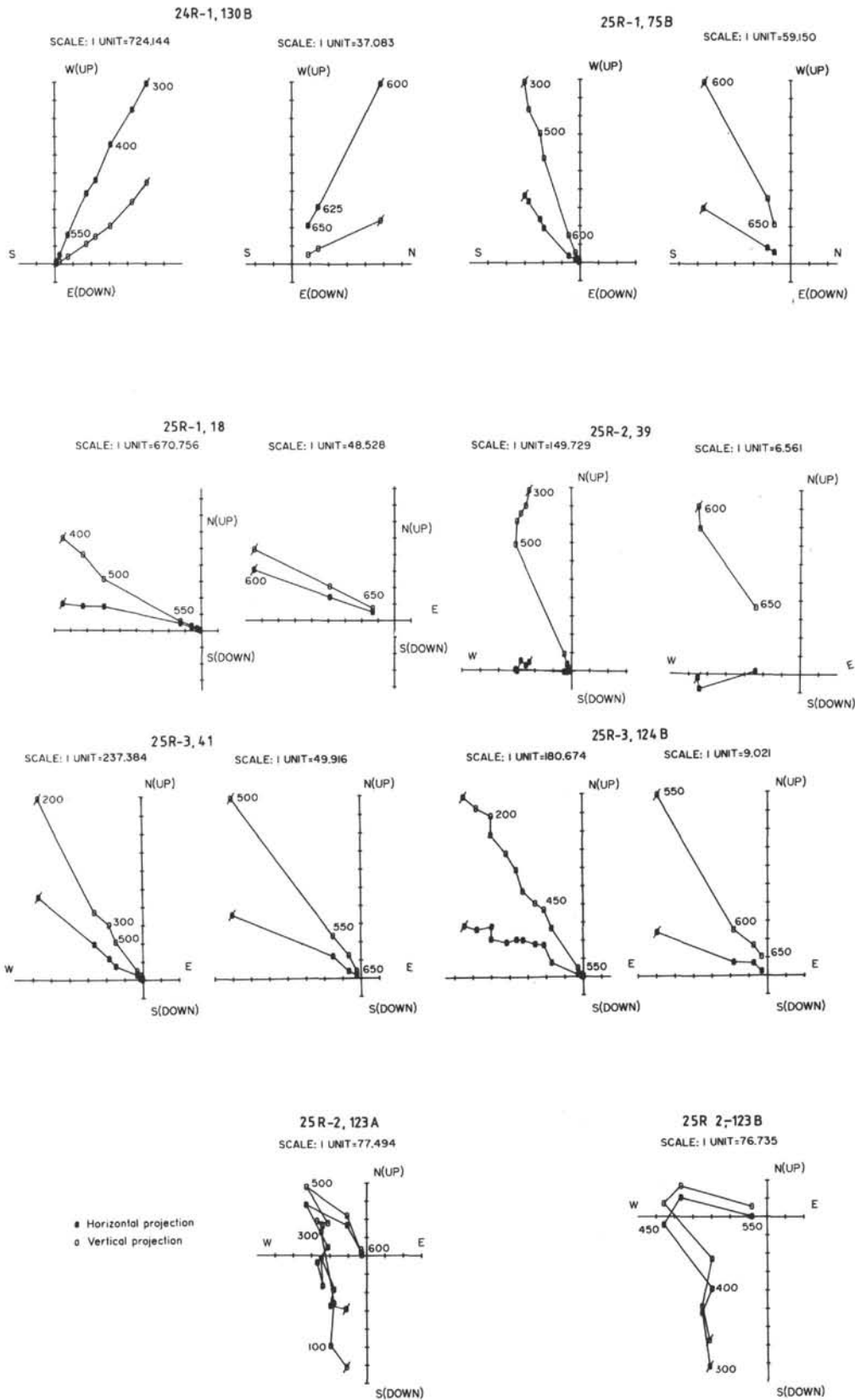


Figure 4. Response of the eight basalt samples from Hole 698A to thermal demagnetization. Symbols and conventions as in Figure 2. Sample 114-698A-25R-2, 123 cm (A), was previously subjected to AF demagnetization in applied fields of up to 30 mT. Numbers refer to demagnetization temperatures (°C). Separate plots for the temperature intervals 300°–575°C and 600°–650°C are shown for most of the samples to illustrate high-temperature behavior.

**Table 2. Principal components of remanent magnetization identified from thermal demagnetization, Hole 698A.**

Core, section, interval (cm)	Unblocking temperature component	Treatment range (°C)	Declination (degrees)	Inclination (degrees)
114-698A-				
24R-1, 130 (B)	Low	300-400	301	-31
	Moderate	400-500	296	-17
	High	600-650	293	-8
25R-1, 1 (B)	Low	400-500	274	-43
	Moderate	500-550	282	-28
	High	600-650	290	-25
25R-1, 75 (B)	Low	300-500	239	-61
	Moderate	500-550	228	-64
	High	625-650	214	-66
25R-2, 39	Low	300-500	42	-66
	Moderate	500-550	273	-66
	High	625-650	257	-54
25R-2, 123 (A)	Low	100-300	167	67
	Moderate	500-550	296	-32
	High	650	257	-46
25R-2, 123 (B)	Low	300-400	181	44
	Moderate	400-450	143	35
	Moderate	500-550	284	-18
25R-3, 124 (B)	Low	200-450	280	-54
	Moderate	500-600	295	-55
	High	625-650	314	-57
25R-3, 41	Low	250-500	316	-43
	Moderate	500-550	293	-52
	High	625-650	301	-58

during this treatment suggests that the low-coercivity component is less homogeneously distributed than the high-coercivity component that remains.

This feature is not seen for the third sample analyzed, 114-698A-25R-1, 75 cm (A), for which there is neither a systematic decrease in the relative second harmonic amplitude (Fig. 6) nor an indication of a significant low-coercivity component of remanence (Fig. 7). The median destructive field (MDF) value for this sample is 27.5 mT, compared with values of 7.5 and 8.5 mT for the other two samples. Thus, the unevenly distributed low-coercivity component appears to be restricted to the latter two samples.

Full appreciation of the significance of these magnetic homogeneity data requires detailed petrological examination of the samples, which is beyond the scope of the present study. However, thin sections prepared from these samples indicate the presence of fractures containing alteration products, including iron oxides, in Samples 114-698A-25R-2, 123 cm (A), and 114-698A-25R-3, 124 cm (A), but not in Sample 114-698A-25R-1, 75 cm (A). It is possible that the unevenly distributed low-coercivity component is carried by multidomain magnetite produced by chemical alteration along these fractures. IRM acquisition analyses show a rapid magnetic saturation of all Hole 698A samples in applied fields of less than 0.2 T (Fig. 8). This indicates that titanomagnetite is likely the dominant magnetic constituent.

### Magnetic Anisotropy

The directions of the maximum and minimum magnetic susceptibility axes for the Hole 698A basalt samples, defined from low-field (10 mT) torque magnetometer measurements, are shown in Figure 9. Histograms of the percentage anisotropy ( $h\%$ ) and anisotropy quotient ( $q$ ) values are displayed in Figure 10. The percentage anisotropy is defined by

$$h\% = \frac{(K_{max} - K_{min}) \times 100}{K_{int}} \quad (1)$$

The anisotropy quotient represents the ratio of the magnetic lineation to the magnetic foliation and is defined by

$$q = \frac{K_{max} - K_{int}}{(K_{max} + K_{int})/2 - K_{min}} \quad (2)$$

where  $K_{max}$ ,  $K_{int}$ , and  $K_{min}$  are the magnitudes of the orthogonal maximum, intermediate, and minimum susceptibility axes, respectively.

For isotropic rocks, in which  $K_{max} - K_{int} = K_{int} - K_{min}$ , the  $q$  value is two-thirds. Lower values represent a dominance of magnetic foliation whilst higher values represent a dominance of magnetic lineation in the magnetic fabric.

Because the principal magnetic constituent of these rocks is titanomagnetite (determined from IRM-acquisition analyses), which is crystallographically isotropic, the observed magnetic fabric is likely to arise from the shape anisotropy of nonequidimensional titanomagnetite grains. Thus, the maximum susceptibility axis will reflect the direction of any preferred orientation of the long axes of these grains and the minimum susceptibility axis that of the short axes. The degree of anisotropy of these rocks is quite low, with most of the  $h$  values <1% (Fig. 10A). The  $q$  values show a wide spread (Fig. 10B) but six of the eight values are <0.67, indicating a dominance of magnetic foliation over lineation. The  $K_{min}$  axes of these six samples group around the vertical (Fig. 9A), indicating that the foliation planes (which are orthogonal to the  $K_{min}$  axes) are near horizontal. The overall mean foliation plane dip for these samples is 14°. The near-horizontal magnetic foliation most likely reflects gravitational settling of the ferromagnetic mineral grains during solidification of the magma.

The maximum susceptibility axes show quite a wide scatter when plotted relative to the arbitrary fiducial direction "F" in each sample (Fig. 9B). However, an estimate of the direction of geographic north at the time of emplacement of the rocks is available from the direction of stable characteristic magnetization in each sample. When the maximum susceptibility axes are plotted relative to this estimate of north (Fig. 9D), there is no apparent reduction in scatter. Thus, no significant magnetic lineation can be identified in these rocks.

There is no apparent correlation between the percentage anisotropy values and the degree of homogeneity of the NRM. The percentage anisotropy (0.6%) of Sample 114-698A-25R-1, 75 cm (A), which showed a relatively low initial relative second harmonic amplitude parameter, is similar to the values (0.7% and 0.3%) for the two samples that showed much higher initial parameters (114-698A-25R-2, 123 cm (A), and 114-698A-25R-3, 124 cm (A)). This probably reflects the dominance of relatively fine magnetic grains as carriers of the NRM and coarser magnetic grains as contributors to the magnetic susceptibility and its anisotropy. Thus, the two properties appear to be largely independent of each other in these rocks.

### PALEOMAGNETIC DIRECTIONAL PROPERTIES OF HOLE 703A BASALT SAMPLES

Only four samples were available for paleomagnetic analysis from the Hole 703A basalts. Of these, three were subjected to incremental AF demagnetization and one to thermal demagnetization (Table 1). The responses to AF demagnetization are shown in Figure 11. Because the magnetic intensity of Sample 114-703A-40X-2, 108 cm, was reduced to <5% of the NRM at an applied field of 20 mT, resulting in poor repeatability, treatment was discontinued at this level. The other two samples were demagnetized up to 30 mT.

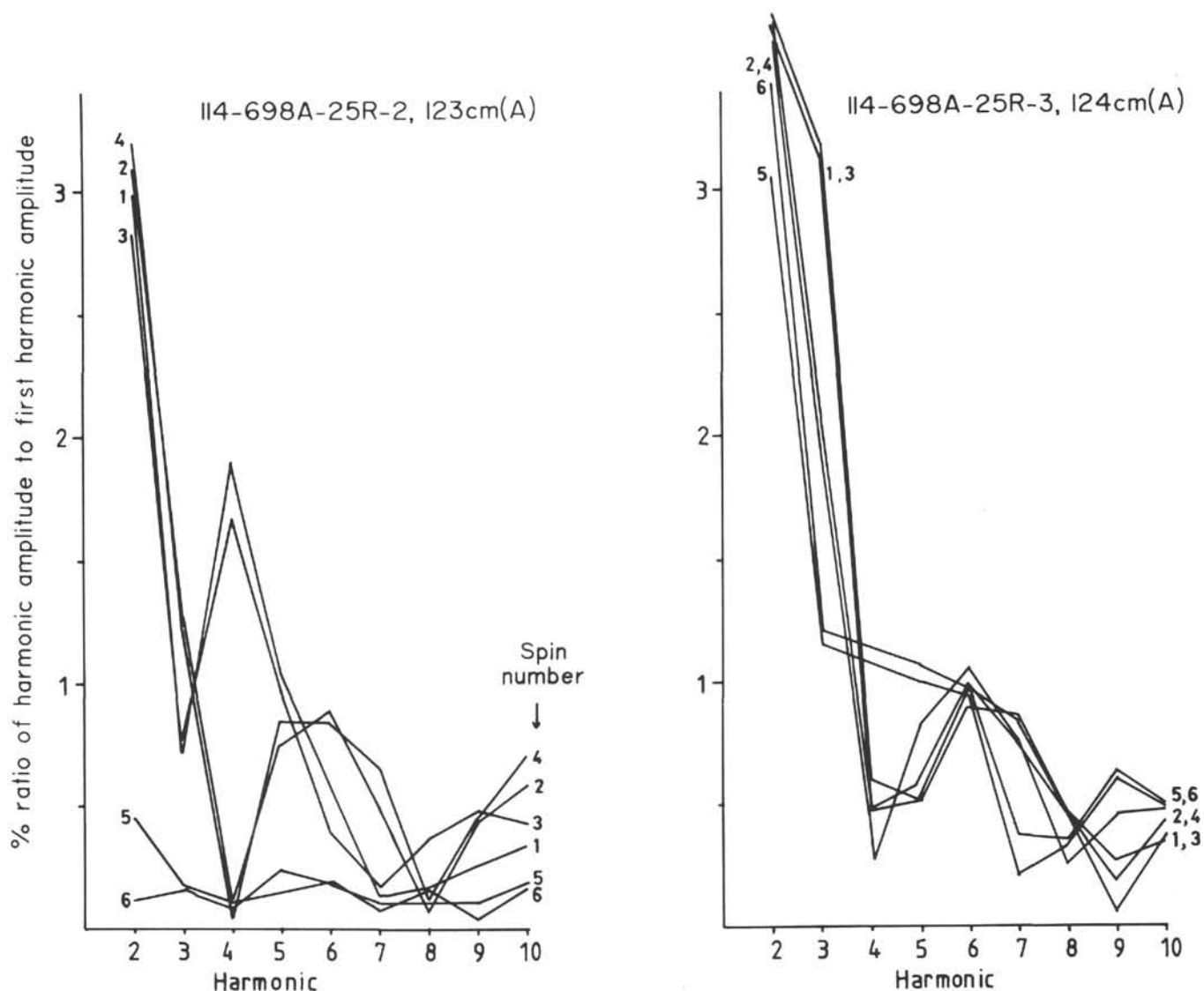


Figure 5. Relative amplitude of the first 10 harmonics determined from Fourier analysis of Molspin magnetometer output for NRM measurements on two representative basalt samples from Hole 698A. The amplitude values are expressed as percentage ratios of the first harmonic amplitude. Numbers refer to the spin axis orientation in the magnetometer. Note the similarity of harmonic content for spins 1 and 3, 2 and 4, and 5 and 6.

Table 3. Magnetization components measured for each spin on the Molspin magnetometer.

Spin number	Magnetization components
1	-y, z
2	-x, z
3	y, -z
4	x, -z
5	x, y
6	-x, -y

As directional trends continued up to the highest demagnetization level, no AF demagnetization stable end point was defined for Samples 114-703A-40X-2, 61 cm (A), and 114-703A-40X-3, 92 cm. Both of these samples carry a reverse polarity (positive inclination) moderate-coercivity component, accompanied by one (or more) low-coercivity ( $H_C$ ) components (Table 4). For the latter sample the magnetic inclination becomes negative during the last two demagnetization

steps (Fig. 11C) indicating the presence of a normal polarity high-coercivity component. A reverse polarity moderate-coercivity component is also present in Sample 114-703A-40X-2, 108 cm (Fig. 11B), but the lack of reliable AF demagnetization data for fields above 20 mT prevents definition of any high-coercivity component in this sample.

Sample 114-703A-40X-2, 61 cm (B), which was subjected to thermal demagnetization (Fig. 11D), shows broadly similar behavior at low demagnetization temperatures (300°C) to its sister Sample 114-703A-40X-2, 61 cm (A), which was subjected to AF treatment (Fig. 11A). However, at temperatures above 350°C the magnetic inclination of this sample becomes negative, indicating the presence of a normal polarity high blocking-temperature component of magnetization. Thus, the combined AF and thermal demagnetization data indicate that the high-stability (high  $T_B$  and  $H_C$ ) components of magnetization in the Hole 703A basalts have a normal polarity, but that a moderately stable reverse polarity component is superimposed on this characteristic component. Unfortunately, the small number of samples and poorly defined demagnetization

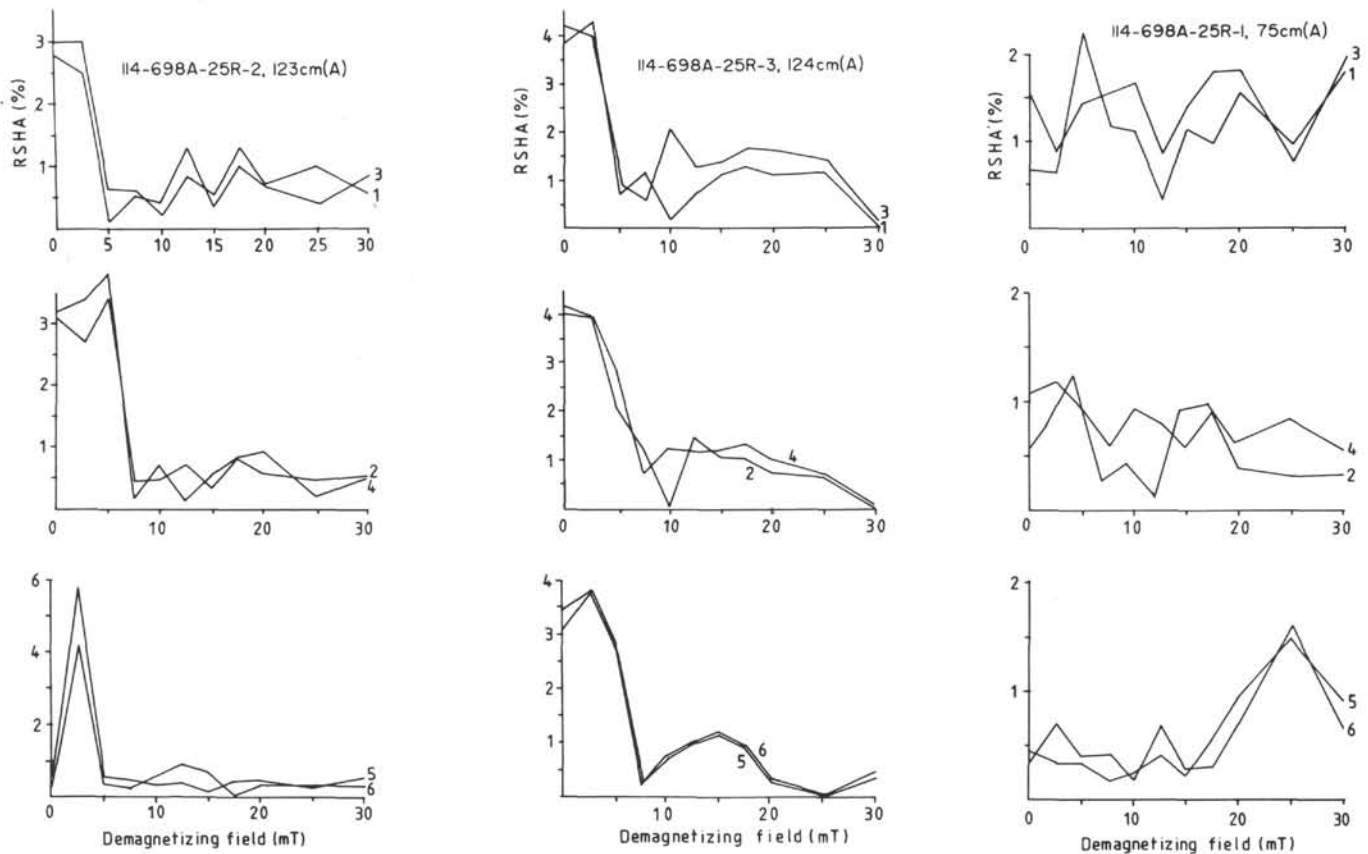


Figure 6. Variation of the relative second harmonic amplitude (RSHA) with AF demagnetization field strength for three basalt samples from Hole 698A. Numbers refer to the spin axis orientation in the magnetometer.

end points preclude precise specification of the direction of the high-stability component.

#### PALEOMAGNETIC DIRECTIONAL PROPERTIES OF HOLE 703A VOLCANIC BRECCIA SAMPLES

The volcanic breccia recovered in Core 114-703A-34X consists of fragments of pumice and volcanic glass shards in a partly cemented state. Although the upper and lower parts of the core were extensively disturbed by drilling, the middle three sections (114-703A-34X-2 to 114-703A-34X-4) were more compact and appeared less disturbed. The remanent magnetism of the archive halves of these three sections was measured aboard *JOIDES Resolution* immediately after cutting, using the shipboard whole-core cryogenic magnetometer system. Both the NRM and the magnetization remaining after partial demagnetization in a field of 5 mT were measured (Fig. 12).

The NRM is characterized by a variable, but mostly steep, negative inclination and an intensity in the range  $10^{-1}$  to  $10^{-2}$  A/m. However, after partial AF demagnetization at 5 mT the intensity is reduced by an order of magnitude and the inclination becomes strongly positive.

These results indicate the presence of a strong normal polarity overprint with a variable direction, possibly acquired in the present geomagnetic field at the drill site, superimposed on a more stable reverse polarity magnetization. The presence of the latter component is surprising, in view of the random orientations of the basaltic fragments within the breccia. If the magnetization of these fragments predated emplacement of the breccia, then their random orientation should result in an incoherent stable remanent magnetization throughout the

core. The presence of a coherent reverse polarity stable magnetization suggests that the whole unit acquired a component of stable magnetization, either through chemical alteration of the breccia during a period of reverse geomagnetic field or through exposure to a strong downward-directed magnetic field in the drill pipe or at some other stage in the drilling and sampling process.

To further investigate the nature of the magnetization in the breccia, paleomagnetic samples were cut from seven pumice pieces from the working half of the core. Two of these samples were cut in half to provide a total of nine samples, six of which were subjected to AF demagnetization. The response to demagnetization was generally erratic and few linear segments could be identified on the vector plots. However, inspection of the stereographic plots showing the directional changes of the magnetic vectors during this treatment (Fig. 13) indicates a clear tendency for the directions to concentrate in the "NW" quadrant, generally with a negative inclination, after demagnetization in fields above about 30 mT. Unfortunately, the samples subjected to thermal demagnetization disintegrated at temperatures in the range of 200° to 300°C, so that treatment at higher temperatures was not possible. However, the general behavior up to these temperatures (Fig. 14) was similar to that during AF demagnetization.

The direction of the high-coercivity component in each sample was estimated by calculating the mean direction for the last few demagnetization steps (generally  $\geq 20$  mT) (Fig. 15).

The most important result of these discrete sample demagnetization analyses is that no evidence was found for the positive inclination (reverse polarity) component identified

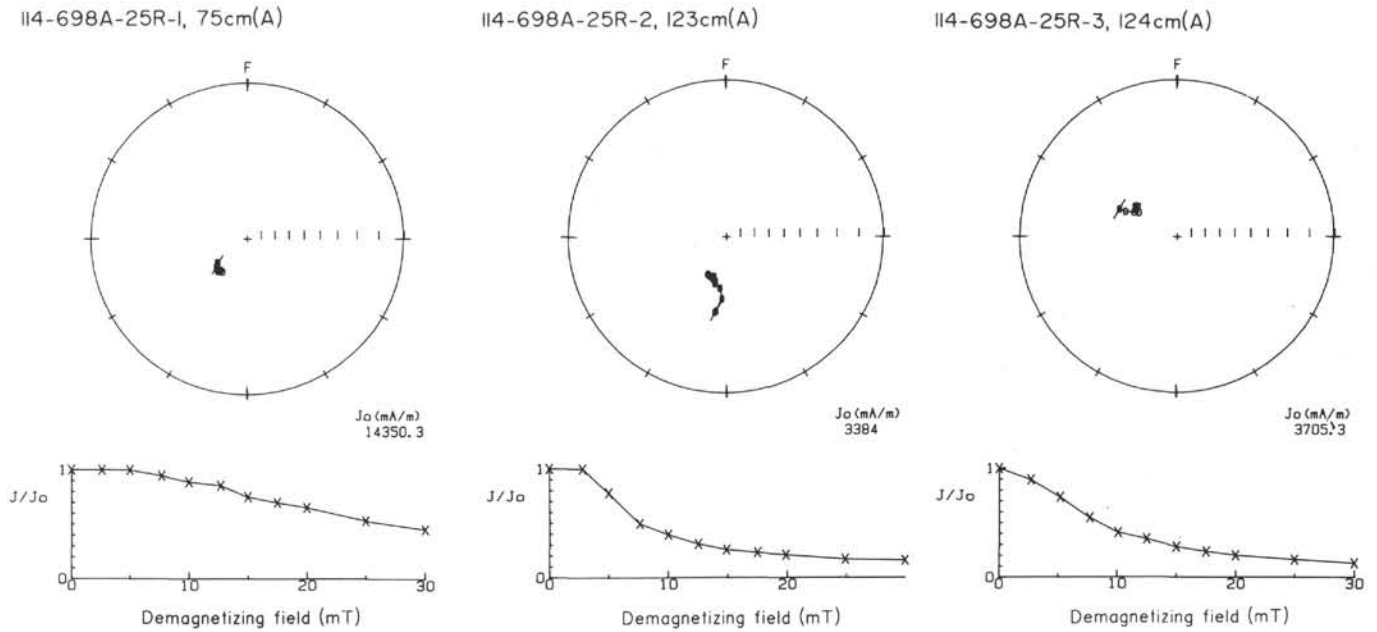


Figure 7. Response of certain Hole 698A basalts to AF demagnetization. Directions are shown on stereographic projections, and intensity ( $J$ ) is shown normalized against the NRM value ( $J_0$ ). Symbols as in Figure 3. Corresponding vector end-point plots for these samples are shown in Figure 2.

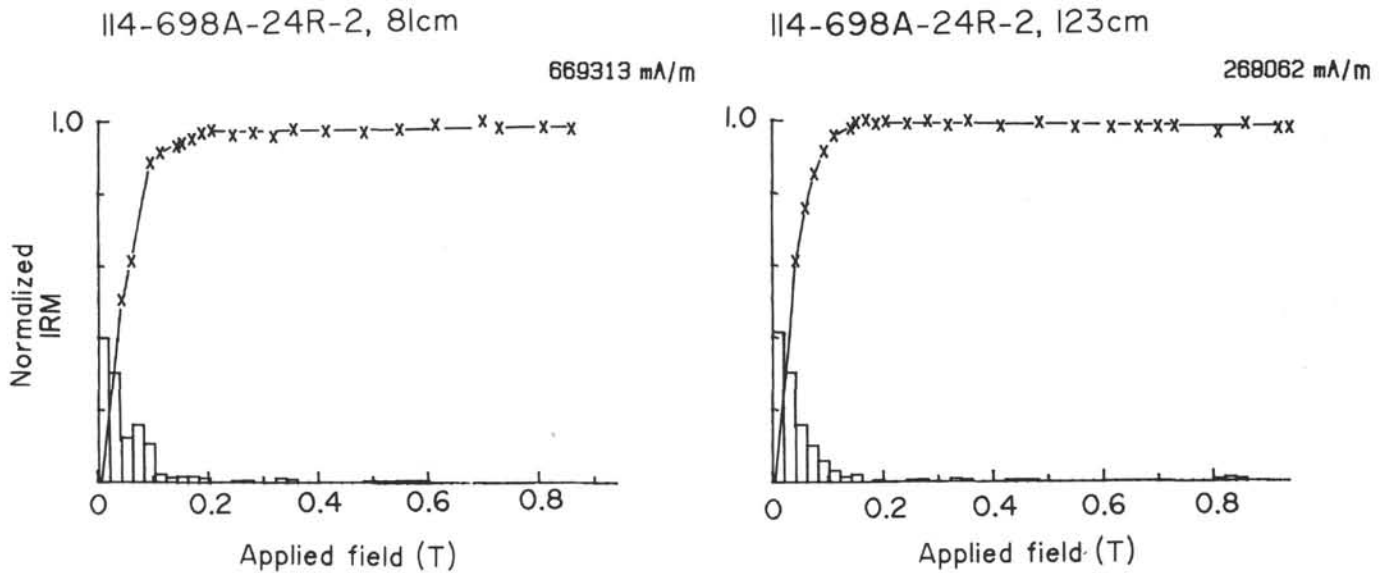


Figure 8. Representative IRM acquisition curves for Site 698 basalts. The saturation IRM value is also shown.

from the shipboard demagnetization of the archive core half at 5 mT. This is surprising, in view of the apparent coherence of this component (Fig. 12). There are at least three possible explanations for the absence of this component in the discrete samples. These involve (1) magnetometer calibration errors, (2) acquisition/decay of viscous magnetizations, and (3) chemical alteration. Magnetometer calibration errors can be ruled out because the calibration of both the shipboard whole-core magnetometer and the shorebased laboratory spinner magnetometer was checked regularly, and excellent agreement between the two instruments was also obtained in concurrent studies of Leg 114 sediments (Hailwood and Clement, this volume).

The second possibility is that the reverse polarity component observed with the whole-core magnetometer represents a viscous remanent magnetization (VRM) or IRM acquired during the drilling process, which had decayed away by the time of the shorebased laboratory measurements, some three months later. A major problem with this interpretation is that a strong normal polarity overprint was observed in the shipboard measurements, superimposed on the reverse polarity component (Fig. 12). This normal overprint likely represents a VRM acquired in the present geomagnetic field at the drill site. If the reverse polarity component were also a VRM (or IRM) acquired, for example, through exposure to a relatively strong downward-directed magnetic field at some point in the drill

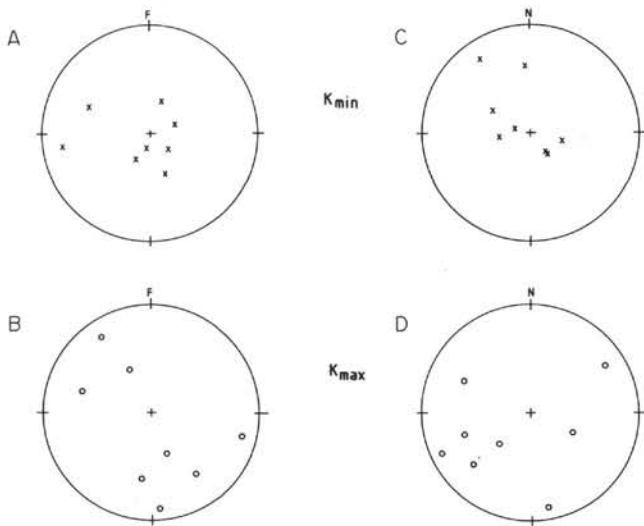


Figure 9. Results of magnetic susceptibility anisotropy (magnetic fabric) determinations on Site 698 basalts plotted as upper hemisphere stereographic projections. A and B. Minimum and maximum susceptibility axes, respectively, plotted relative to the arbitrary fiducial azimuth in each piece of core. C and D. Minimum and maximum susceptibility axes, respectively, plotted relative to the direction of geographic north in each sample defined from the declination of the stable characteristic magnetization.

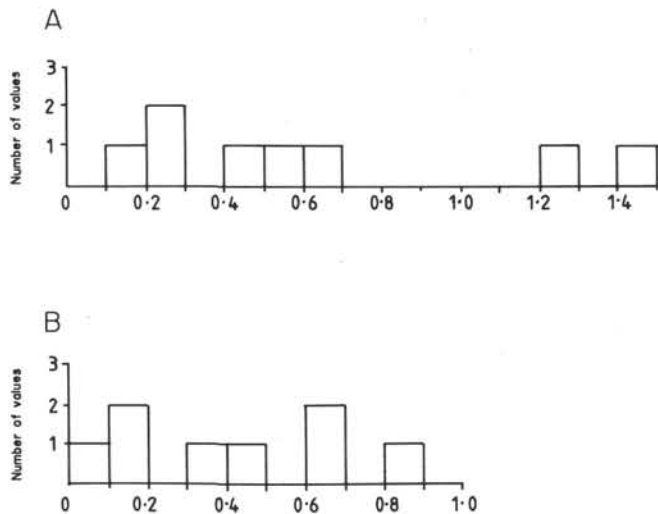


Figure 10. Histograms of (A) percentage anisotropy and (B) anisotropy quotient values for Hole 698A basalts.

pipe or during subsequent handling of the core, then this component would be expected to replace the earlier normal polarity VRM, rather than to coexist with it. An assessment of the possible importance of VRM in these rocks was made from a consideration of their general magnetic stability, revealed from laboratory incremental demagnetization and also from laboratory VRM decay experiments. Useful parameters obtained from the laboratory AF demagnetization include the MDF values (the demagnetization field at which the magnetic intensity is reduced to 50% of the initial NRM value) and the values of the RRM ratio (see "Paleomagnetic Investigations" section).

The MDF values for the Hole 703A breccia samples are very low ( $\leq 5$  mT; Table 5), particularly in comparison with

values for the Hole 698A basalts. The RRM ratios are similarly very high, typically  $\sim 10\%$ – $90\%$  (Fig. 16), indicating that these samples are particularly prone to acquiring spurious rotational remanent magnetization during AF demagnetization. Together, these two results indicate that the Hole 703A volcanic breccia samples contain significant proportions of low-coercivity magnetic grains, which will be susceptible to acquiring VRMs, either at the drill site or during laboratory storage.

An attempt was made to obtain a more direct measure of the magnetic viscosity of these samples (and also that of the Hole 703A basalt samples) by storing representative samples in field-free space (within a triple-layer Mu-metal box with a residual field of  $< 50$  nT) for periods up to 1100 hr and monitoring the change in magnetic intensity at regular intervals. The results of these experiments are shown in Figure 17 as plots of the normalized intensity ( $J/J_0$ ) vs. log time. A certain amount of noise is present in these curves, probably due to exposure of the samples to the geomagnetic field in the laboratory during transfer from the Mu-metal box to the shielded environment of the magnetometer prior to measurement. However, an overall reduction of magnetic intensity with time is evident for three of the four breccia samples and for all three of the basalt samples. This approximately linear relationship between magnetization and log time indicates an overall exponential decay of the magnetization within the field-free space. The decay rate can be represented by the viscosity coefficient  $S$ , derived from the relationship

$$VRM(t) = J(t) - J(0) = S \log t, \quad (3)$$

where  $J(0)$  is the initial magnetic intensity and  $J(t)$  is the value after time  $t$  (Lowrie et al., 1983).

The values of  $S$  obtained for these samples are listed in Table 6, together with the estimated intensities of VRM that would be acquired by the samples over different periods of time, assuming that the rate of growth of the VRM in the geomagnetic field is comparable to the rate of decay of the NRM observed in these experiments. It is clear that typically  $\sim 30\%$  of the original NRM of the samples may decay (or be replaced) over a three-month period. This is considered insufficient to explain the complete removal and/or replacement of the relatively stable reverse polarity component defined from the shipboard analyses during the three-month period prior to the shorebased laboratory measurements (during which time the samples were stored in random orientations in the laboratory geomagnetic field).

A third explanation for the disappearance of the reverse polarity component is that the samples underwent chemical changes during storage and partial drying out in the laboratory, resulting in the destruction or modification of the ferromagnetic mineral grains carrying the reverse polarity component. Because the samples were stored in air, in a markedly different geochemical environment from that of their original seafloor location, such changes are quite possible. However, the original magnetomineralogy of the rocks is unknown, and detailed geochemical/magnetomineralogical studies of their present state were not possible within the scope of this investigation. Limited information on the magnetomineralogy was obtained from the analysis of IRM acquisition on two samples (Fig. 18). In both cases the magnetization saturates in very weak applied fields ( $\leq 0.1$  T), indicating that the dominant magnetic mineral present is titanomagnetite. There is no evidence for a further progressive increase in magnetization at higher fields, which might indicate the presence of hematite. This is a surprising result, in view of the highly

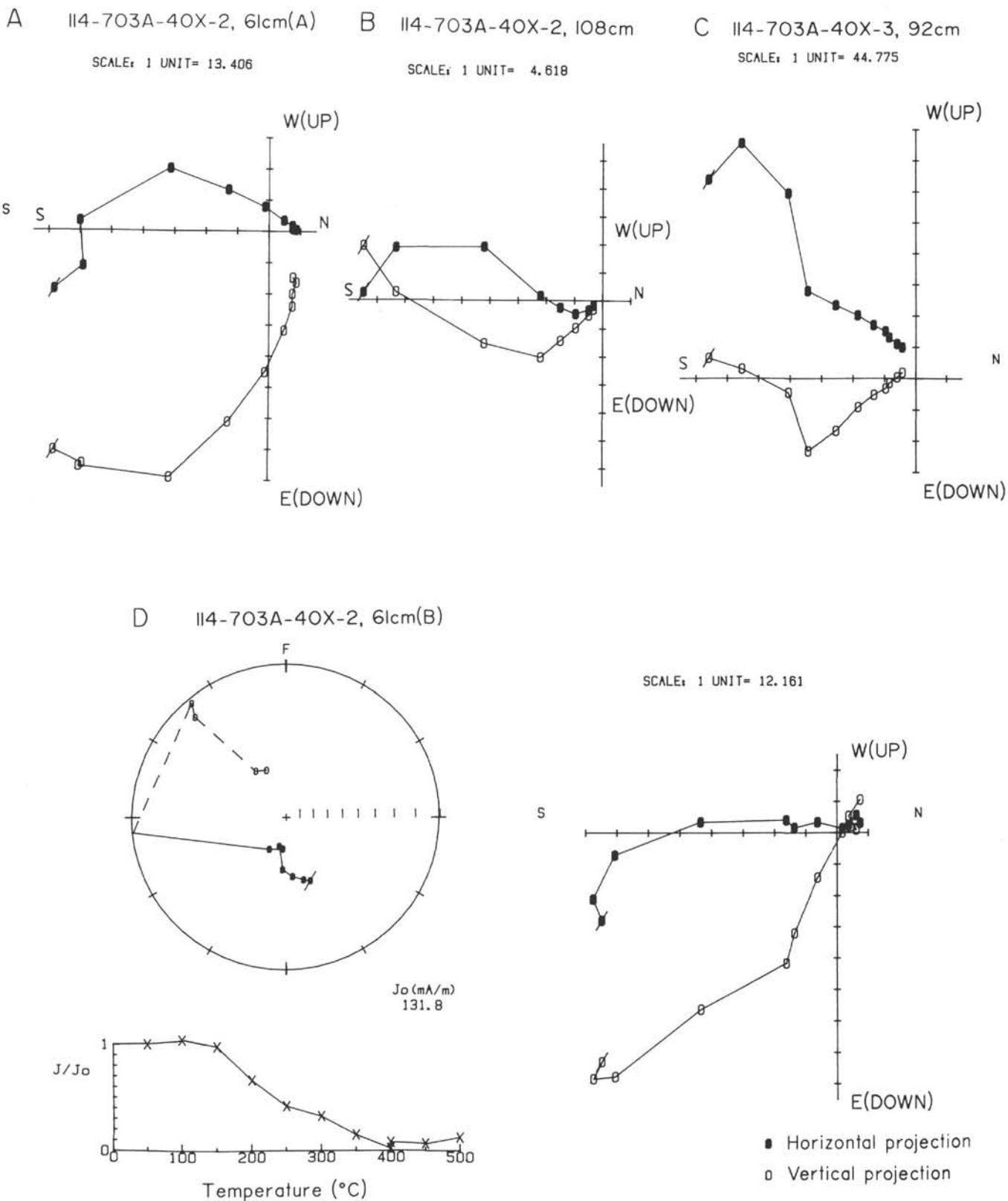


Figure 11. Response of basalt samples from Hole 703A to (A-C) AF demagnetization and (D) thermal demagnetization. Symbols as in Figures 2 and 3.

**Table 4. Magnetization components in Hole 703A basalt samples.**

Core, section, interval (cm)	Component <sup>a</sup>	Treatment range	Declination (degrees)	Inclination (degrees)
114-703A-40X-2, 61 (A)	Low $H_C$	7.5–10 mT	200	42
	Moderate $H_C$	17.5–25 mT	218	74
40X-2, 108	Low $H_C$	7.5–10 mT	211	36
	Moderate $H_C$	15–17.5 mT	147	41
40X-3, 92	Low $H_C$	7.5–17.5 mT	208	37
	Moderate $H_C$	17.5–30 mT	223	33
40X-2, 61 (B)	Low $T_B$	150°–250°C	168	33
	Moderate $T_B$	300°–400°C	181	64
	High $T_B$	450°–500°C	308	–47

<sup>a</sup>  $T_B$  = blocking temperature;  $H_C$  = coercivity.

weathered, overall yellow/brown appearance of the breccia. The mean NRM intensity value obtained from the discrete sample measurements (13.17 mA/m) is the same order of magnitude as that obtained from the shipboard whole-core measurements (~50 mA/m). Thus, it seems likely that much of the titanomagnetite was already present in the breccia at the time of drilling, although the additional production of small amounts by subsequent chemical alteration cannot be ruled out.

As the samples were stored in random orientations, any new magnetization produced by post-drilling alteration should differ from sample to sample. Thus, the consistent normal polarity component with a northwesterly declination and moderate negative inclination, identified from the shorebased laboratory discrete sample measurements (Fig. 15), must have been present before storage and is unlikely to have been produced by chemical alteration.

In summary, three distinct components of magnetization, each consistent between different breccia clasts, were identified in the Hole 703A pumice breccia. The magnetically softest component was removed by shipboard AF demagnetization at 5 mT of the archive core halves and probably represents a viscous component acquired in the present geomagnetic field at the drill site. The intermediate coercivity component, which remained in the archive core halves after 5-mT demagnetization, is reverse polarity, but was destroyed, most likely by chemical alteration, by the time the discrete samples were measured in the Southampton laboratory. A poorly defined weak normal polarity component remains in these samples, and its consistency between samples indicates that it also was present in the breccia at the time of drilling. Clearly the breccia has had a complex history of magnetization and remagnetization prior to drilling, probably representing hydrothermal circulation processes, but the time of acquisition of

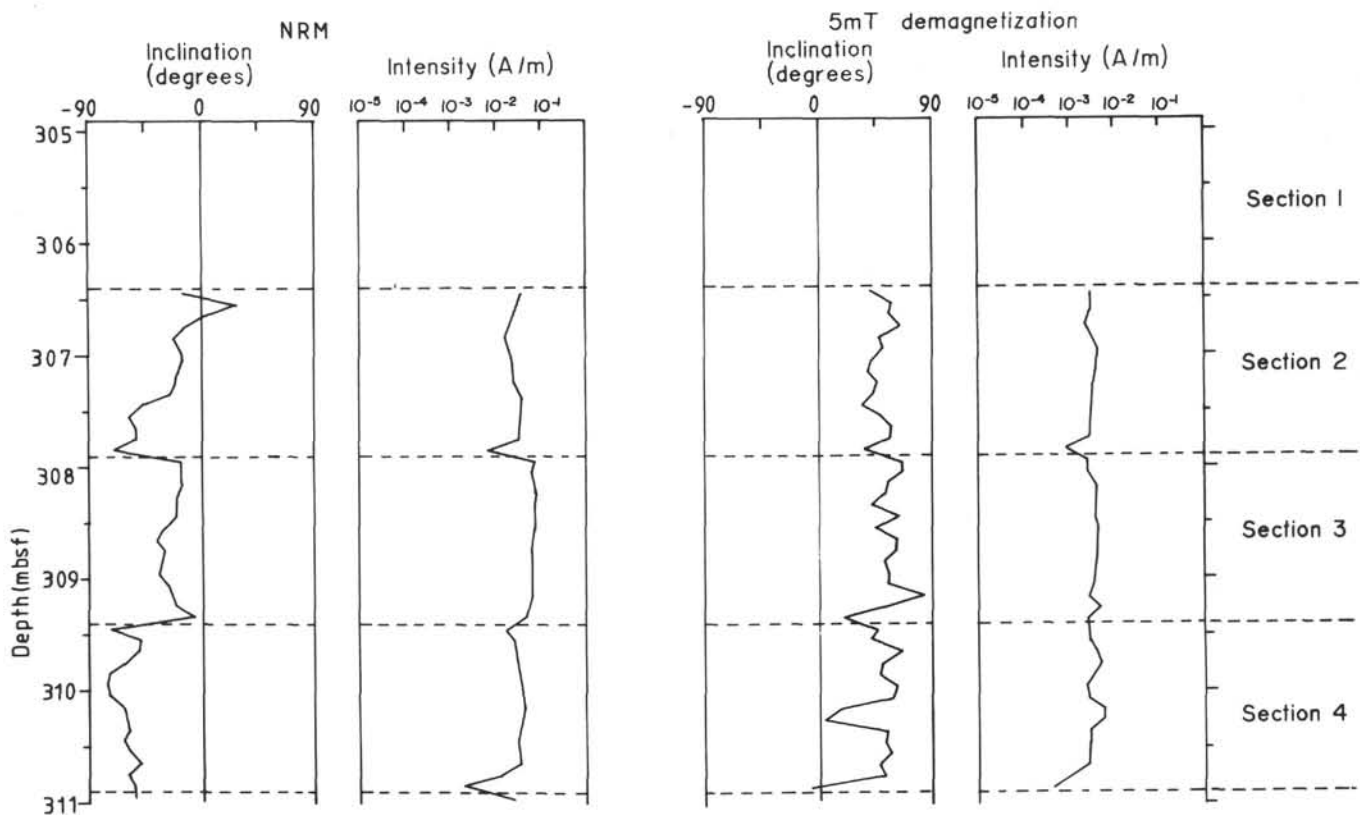


Figure 12. Variation of magnetic inclination and intensity in Sections 114-703A-34X-2 through 114-703A-34X-4, as determined from shipboard whole-core cryogenic magnetometer measurements. Values are shown for the NRM and after AF demagnetization at 5 mT.

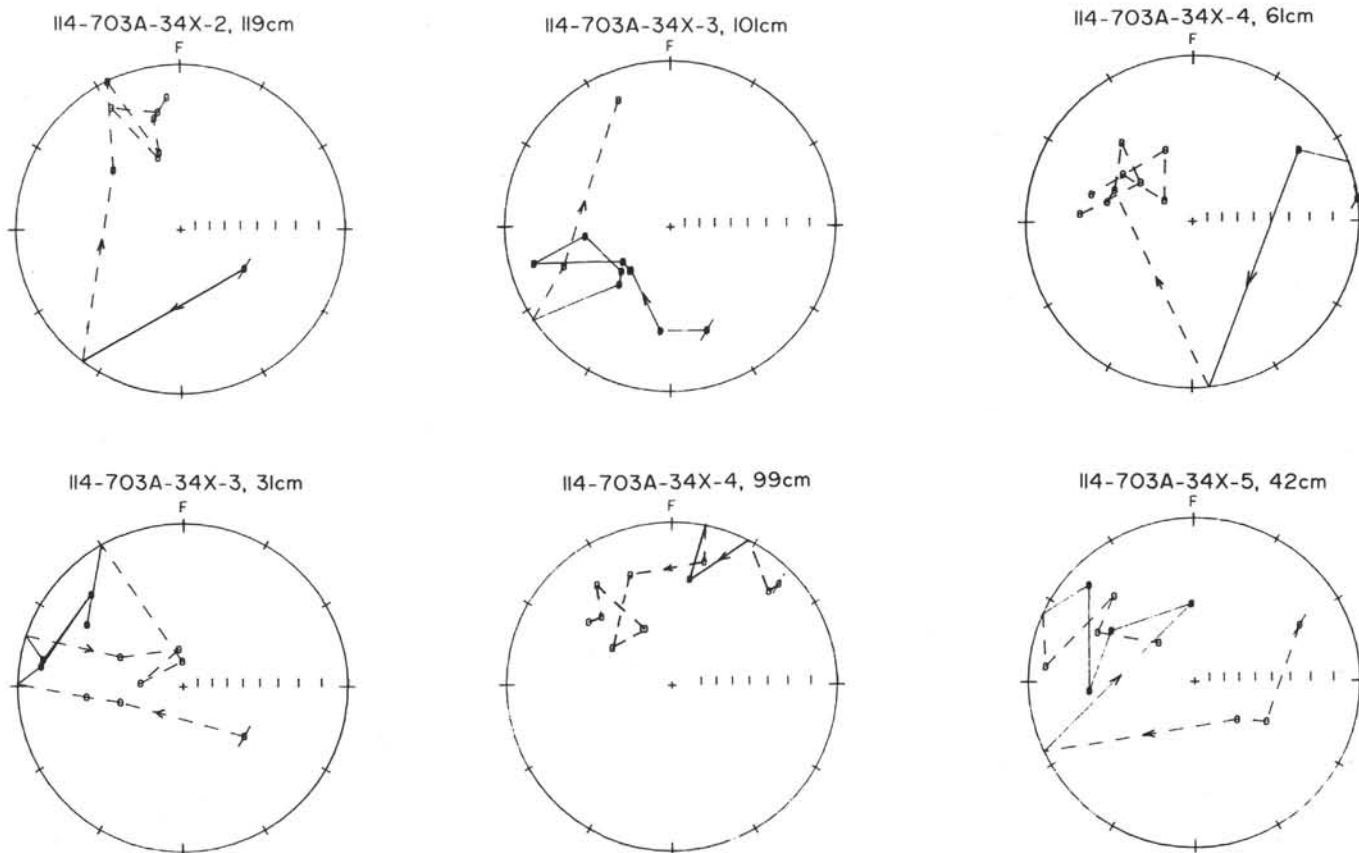


Figure 13. Directional response of Hole 703A volcanic breccia samples to AF demagnetization. Conventions and symbols as in Figures 2 and 7. Demagnetization field values are 2.5, 5, 7.5, 10, 15, 20, 25, 30, and 35 mT.

the observed normal and reverse polarity stable components cannot be determined from the available data.

### MAGNETIC SUSCEPTIBILITY

Histograms of the magnetic susceptibility, Koenigsberger ratio ( $Q_n'$ ), and MDF values for the Hole 698A basalt and the Hole 703A basalt and volcanic breccia samples are shown in Figure 19. There is a clear separation between the relatively high susceptibilities of the Hole 698A basalts and the lower values for the Hole 703A breccias.  $Q_n'$  represents the ratio between the remanent magnetization (represented by the NRM intensity) and the induced magnetization in a field of  $10^{-4}$  T (1 Oe), which is the order of magnitude of the geomagnetic field at the drill site. The induced magnetization is controlled by the magnetic susceptibility.

In all of the Hole 698A basalt samples the remanent magnetization dominates (because  $Q_n' > 1$ ), whilst in the Hole 703A basalt and breccia samples the induced magnetization dominates ( $Q_n' < 1$ ). Thus, the remanent magnetization of the Hole 698A basalt is likely to contribute to observed marine magnetic anomalies whilst that of the Hole 703A basalt and breccia is not.

The relatively low magnetic stability of the Hole 703A volcanic breccia is emphasized by its low MDF values (Fig. 19C).

Plots of MDF vs. susceptibility for oceanic basalts (e.g., Petersen and Roggenthen, 1980; Levi, 1983) commonly show an inverse relationship between these two parameters. This may be explained by changing physical parameters, such as grain size, in a unimodal iron oxide system or, alternatively, by changing composition. In general, larger multidomain

ferromagnetic grains will contribute most to the susceptibility whilst smaller single-domain grains will contribute most to the magnetic stability (and high MDF values). The Leg 114 basement rock MDF values plotted against susceptibility in Figure 20 are in general agreement with the field indicated for East Pacific basalt samples (Petersen and Roggenthen, 1980), but the points on the diagram for the Hole 698A volcanic breccia lie well below the general basalt field. This reflects a combination of low susceptibility and low magnetic stability of the volcanic breccia. Clearly the magnetic properties of this rock are not in any way typical of those of normal oceanic basement rocks.

### MAGNETIC INTENSITY

The NRM intensity values for the 18 samples analyzed are listed in Table 5. There is a clear distinction at Hole 698A between the relatively high intensities of the upper four samples and the rather lower values for the lower four samples.

In order to compare the observed values with those measured at other localities, the values were reduced to the equator using an axial dipolar field model, such that

$$I_{equ} = I_{\lambda} / \sqrt{1 + 3 \sin^2 \lambda}, \quad (4)$$

where  $I_{\lambda}$  is the observed intensity at latitude  $\lambda$ , and  $I_{equ}$  is the corresponding value reduced to the equator.

The geometric mean equatorially-reduced values are listed in Table 5. The mean for the Hole 703A basalts is more than an order of magnitude weaker than that for the Hole 698A

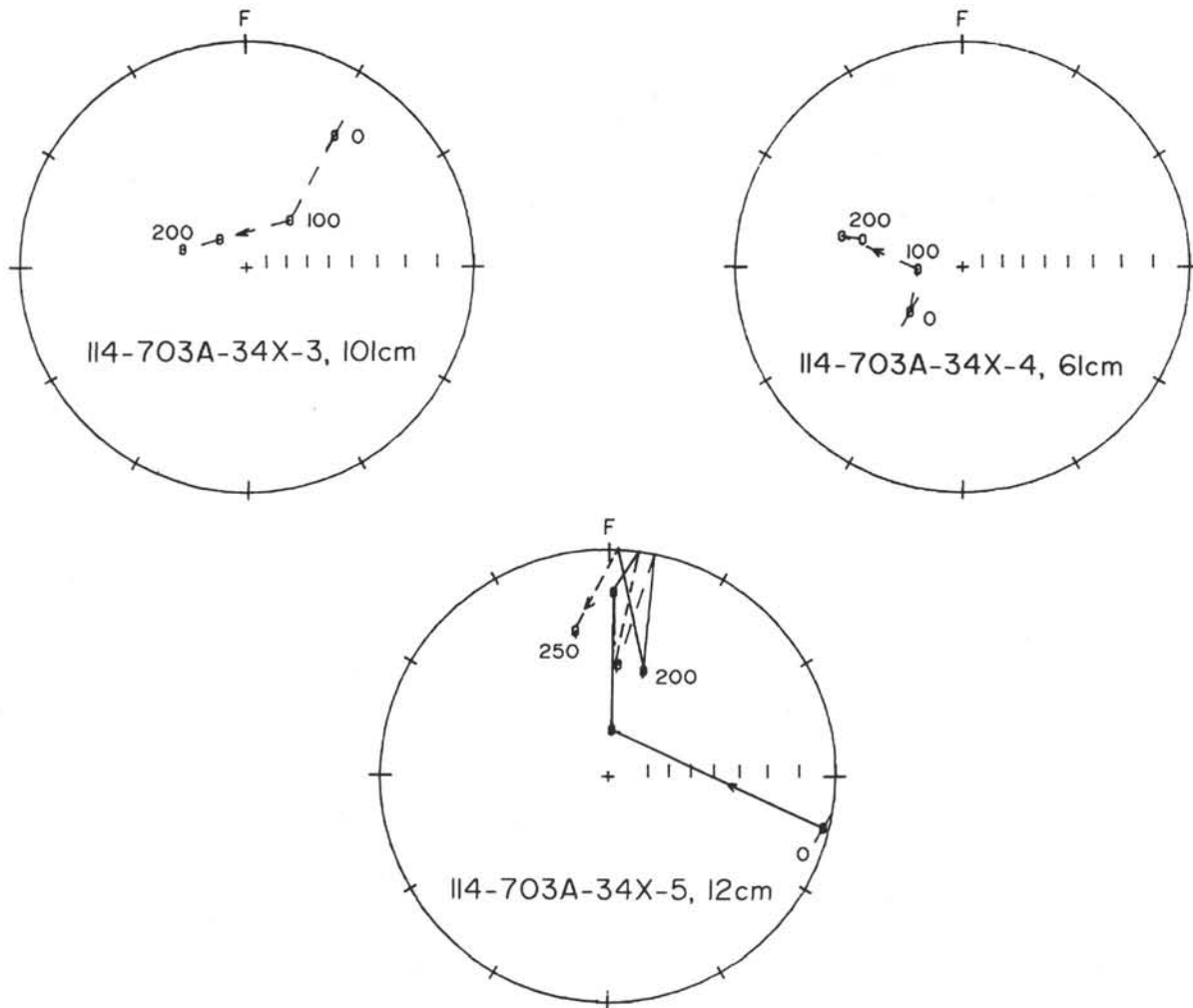


Figure 14. Directional response of Hole 703A volcanic breccia samples to thermal demagnetization. Conventions and symbols as in Figure 7. Numbers represent demagnetization temperature in °C.

basalts, and that for the Hole 703A volcanic breccia is weaker by a further order of magnitude.

Syntheses of magnetic intensity data for oceanic basement rocks (e.g., Irving et al., 1970; Klitgord et al., 1975; Lowrie, 1977; Harrison, 1981) indicate a progressive decrease in magnetic intensity away from the ridge crest (i.e., with increasing age) in all ocean basins. Bleil and Petersen (1983) demonstrated that the decrease, which is initially sharp, occurs out to a crustal age of about 20 Ma, after which the intensity gradually increases again to an age of at least 120 Ma. The mean value at the ridge crest is typically ~5 A/m whilst that at 20 Ma is ~1 A/m, rising to about 4 A/m at 120 Ma. Magnetomineralogical investigations indicate that the initial decrease is due mainly to the progressive low-temperature oxidation of the stoichiometric titanium-rich titanomagnetite. Bleil and Petersen (1983) suggested that the subsequent increase in magnetic intensity with age may be due to Fe migration out of the tetrahedral sites of the titanomagnetite spinel lattice or inversion of the metastable cation-deficient titanomaghemite to an intergrowth of mag-

netite and other stable Fe-Ti oxides. However, the progressive increase requires that this inversion preserve the original direction of magnetization.

The most useful indicator of the magnetomineralogical composition of submarine basalts is the Curie temperature, determined from thermomagnetic analysis. Thus, the Curie temperature of completely unaltered submarine basalt is typically ~125°C, corresponding to a composition of  $\text{Fe}_{2.27}\text{Ti}_{0.58}\text{Al}_{0.07}\text{Mg}_{0.06}\text{Mn}_{0.02}\text{O}_4$ . An increase in the degree of low-temperature oxidation is accompanied by an increase in Curie temperature.

Unfortunately, as thermomagnetic analyses of the Leg 114 basement rocks were not possible within the scope of the present study, the degree of oxidation of these rocks remains uncertain. Some information is available from the intensities of magnetization (Table 5). The upper 3.5 m of the Hole 698A basalt section has a much higher magnetic intensity than the underlying 2.3 m. If these basalts belong to a single cooling unit then this difference could be explained by the upper part representing a more rapidly quenched (and finer-grained)

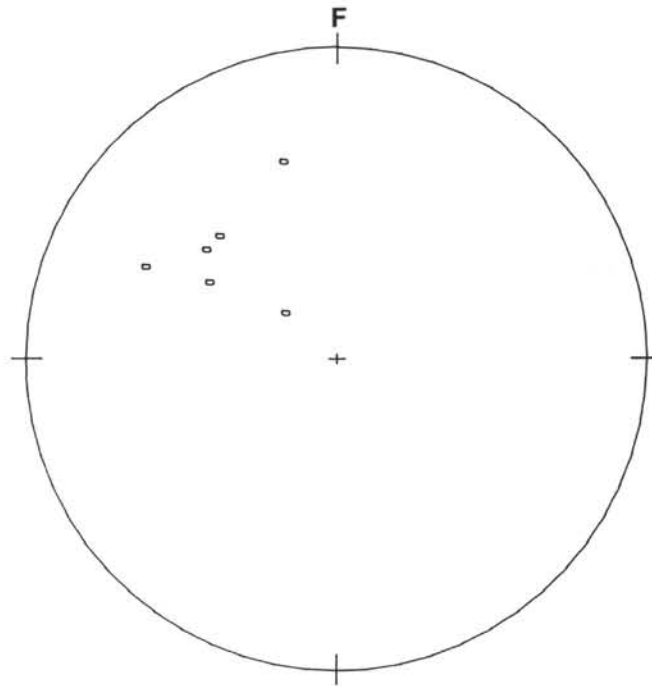


Figure 15. Directions of high-coercivity vectors for Hole 703A volcanic breccia samples from Core 114-703A-34X in stereographic projection. Symbols as in Figure 3.

Table 5. Magnetic intensity, susceptibility, Koenigsberger ratio, and MDF values, Leg 114.

Core, section, interval (cm)	Magnetic intensity (mA/m)	Equatorial J (mA/m)	Geometric mean (mA/m)	Volume susceptibility (SI $\times 10^{-3}$ )	Koenigsberger ratio	MDF (mT)
Basalt						
114-698A-24R-1, 30	14,377	8653	↑	24.3	7.44	27
24R-2, 81	21,882	13170		24.8	11.08	25
25R-1, 18	12,894	7760	9854	28.6	5.66	—
25R-1, 75	16,335	9832	↓	27.3	7.52	27.5
25R-2, 39	5226	3145	↑	33.3	1.97	—
25R-2, 123	3504	2109	↓	20.4	2.16	7.5
25R-3, 41	3696	2224	2525	37.1	1.25	8.5
25R-3, 124	4577	2754	↓	26.5	2.17	—
114-703A						
40X-2, 61	263.8	158.8	↑	4.6	0.72	12
40X-2, 108	61.7	37.1	125.2	0.9	0.86	6
40X-3, 92	553.3	333.0	↓	26.9	0.26	9
Breccia						
114-703A-34X						
34X-2, 119	41.2	24.8	↑	3.5	0.15	—
34X-3, 31	25.1	15.1		4.4	0.07	5
34X-3, 101	15.9	9.57	13.17	4.7	0.04	2
34X-4, 60	19.9	11.98		2.4	0.10	5
34X-4, 99	19.2	11.56	↓	1.9	0.13	2
34X-5, 12	37.5	22.57	↓	2.8	0.17	3.5
34X-5, 42	10.2	6.14		1.9	0.07	—

exterior and the lower part a more slowly cooled (and coarser-grained) interior. However, preliminary thin-section analyses do not indicate any systematic difference in the grain size of the two parts. Other factors that could contribute to this intensity difference include small variations in the concentration of magnetic minerals and in the degree of oxidation within the unit.

The overall equatorially-reduced mean intensity for this unit is 5.6 A/m, which is just within the range expected for Late Cretaceous age seafloor (1.5 to 5.7 A/m) and is considerably higher than the typical range of values for Tertiary seafloor (Bleil and Petersen, 1983). Thus, these results support the interpretation of the Hole 698A basalts as true basement rocks, rather than a younger intrusion emplaced into overlying

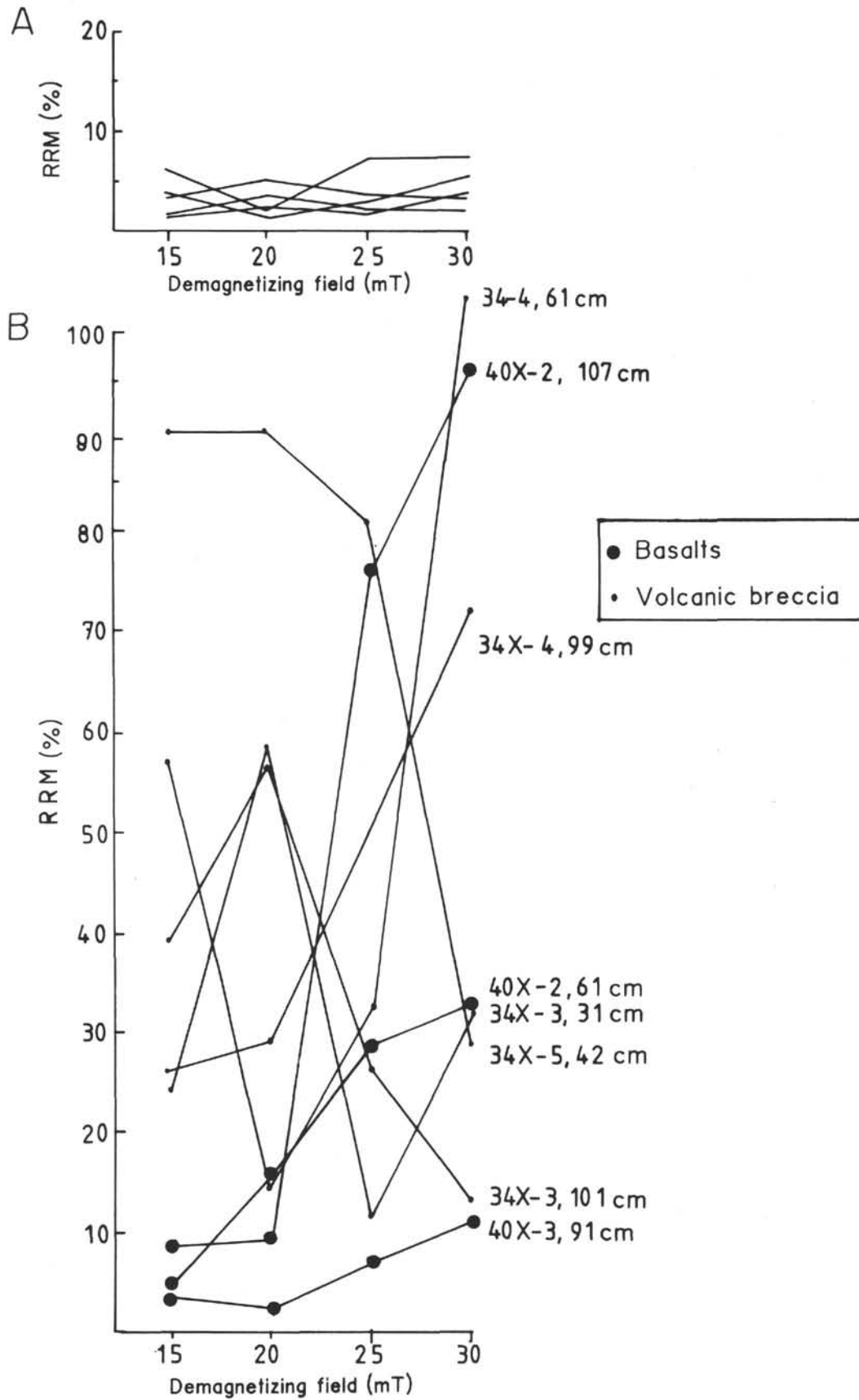


Figure 16. Variation of RRM intensity with the demagnetizing field for (A) Hole 698A basalts and (B) Hole 703A basalts and volcanic breccia. The RRM is represented as a percentage ratio of the NRM after each successive demagnetization step.

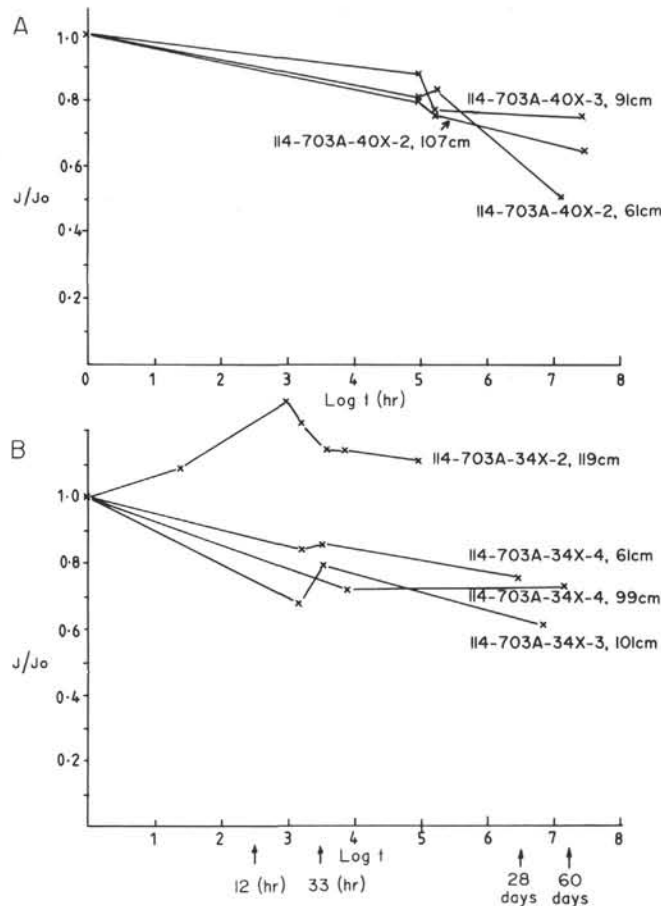


Figure 17. Decay of NRM with time for (A) three Hole 703A basalt samples and (B) four Hole 703A volcanic breccia samples when stored in field-free space within a triple-layer  $\mu$ -metal box.

sediments. The IRM-acquisition curves (Fig. 8) indicate the presence of magnetite, as would be expected from the alteration model of Bleil and Petersen (1983) for rocks of this age.

Hole 703A magnetic intensity data are available only for three basalt samples and it is uncertain how representative these results are. However, all three values are anomalously low, possibly suggesting an unusually high degree of alteration of the original ferromagnetic minerals in this basalt. The magnetic intensity of the overlying volcanic breccia is also very weak, but this may reflect a difference in original composition from that of the basalt.

Table 6. Viscosity parameters, Hole 703A.

Core, section, interval (cm)	Viscosity coefficient	Predicted VRM acquisition (mA/m)			NRM (mA/m)
		3 mo.	1 yr	1 m.y.	
114-703A-					
Basalt					
40X-2, 61	24.73	188.2	222.4	564.1	264
40X-2, 108	2.80	21.3	25.2	63.9	62.0
40X-3, 92	19.12	145.5	172.0	436.1	553.0
Volcanic breccia					
34X-3, 101	0.89	6.8	8.0	20.3	15.9
34X-4, 60	0.80	6.1	7.2	18.2	19.9
34X-4, 99	0.72	5.5	6.5	16.4	19.2

DISCUSSION AND CONCLUSIONS

In view of the poor definition of the directions of the stable magnetic vectors for the Hole 703A basalt and volcanic breccia, it is not possible to make meaningful paleolatitude estimates for this site. The magnetic vectors for the Hole 698A basalts are better defined, and histograms of the inclination values for the low, moderate, and high blocking-temperature components are shown in Figure 21. The bimodal distribution of the low and moderate  $T_B$  components reflects magnetic overprints in some samples. Three of the high  $T_B$  vectors show low inclination values, which may also reflect the presence of such components. The other five vectors, however, form a separate symmetrical distribution with an overall mean inclination value of  $59^\circ \pm 5^\circ$ . The corresponding paleolatitude (calculated from an axial geocentric dipole field model) is  $40^\circ \pm 5^\circ$ , whereas the present site latitude is  $51^\circ\text{S}$ . Because of the small number of determinations contributing to this mean, its precision is unlikely to be high. However, the results indicate that Site 698 may have undergone a southward translation through some  $11^\circ \pm 5^\circ$  of latitude since the Late Cretaceous. This result is broadly compatible with the plate tectonic reconstruction of the South Atlantic area presented by LaBrecque and Hayes (1979), according to which the pivoting action involved in the rotation of South America and the Falkland Plateau away from southern Africa and the Agulhas Plateau results in a net southward movement of the Northeast Georgia Rise through some  $5^\circ$  of latitude.

The polarity of the stable remanent magnetism in the Hole 703A basalts and breccia is poorly defined. The Hole 698A basalts carry a well-defined normal polarity stable characteristic magnetization, which is consistent with the normal polarity observed in the basal sediments, of Campanian age, at this site (Clement and Hailwood, this volume) and the emplacement of the basalt during the long Campanian to early Maestrichtian normal polarity Chron C33N.

REFERENCES

Bleil, U., and Petersen, N., 1983. Variations in magnetization intensity and low-temperature titanomagnetite oxidation of ocean floor basalts. *Nature*, 301:384-388.

Dunlop, D. J., 1979. On the use of Zijderveld vector diagrams in multicomponent paleomagnetic studies. *Phys. Earth Planet. Inter.*, 20:12-24.

Harrison, C.G.A., 1981. Magnetism of the oceanic crust. In Emiliani, C. (Ed.), *The Sea* (vol. 7): New York (Wiley), 219-239.

Hillhouse, J. W., 1977. A method for the removal of rotational remanent magnetization acquired during alternating field demagnetization. *Geophys. J. R. Astron. Soc.*, 50:29-34.

Irving, E., Park, J. K., Haggerty, S. E., Aumento, F., and Loncaravek, B., 1970. Magnetism and opaque mineralogy of basalts from the Mid-Atlantic Ridge at  $45^\circ\text{N}$ . *Nature*, 228:974-976.

Klitgord, K. D., Huestis, S. P., Mudie, J. D., and Parker, R. L., 1975. An analysis of near-bottom magnetic anomalies: sea-floor spreading and the magnetized layer. *Geophys. J. R. Astron. Soc.*, 43:387-424.

LaBrecque, J. L., and Hayes, D. E., 1979. Seafloor spreading history of the Agulhas basin. *Earth Planet. Sci. Lett.*, 45:411-428.

Levi, S., 1983. Paleomagnetism and rock magnetism of submarine basalts from the Galapagos spreading centre near  $86^\circ\text{W}$ . In Honnorez, J., von Herzen, R. P., et al., *Init. Repts. DSDP, 70*: Washington (U.S. Govt. Printing Office), 429-435.

Lowrie, W., 1977. Intensity and direction of magnetization in oceanic basalts. *J. Geol. Soc. London*, 133:61-82.

Lowrie, W., Løvlie, R., and Opdyke, N. D., 1983. Magnetic properties of Deep Sea Drilling Project basalts from the North Pacific Ocean. *J. Geophys. Res.*, 78:7647-7660.

Petersen, N., and Roggenthen, W. M., 1980. Rock and paleomagnetism of Leg 54 basalts—East Pacific Rise and Galapagos areas. In Rosendahl, B. R., Hekinian, R., et al., *Init. Repts. DSDP*, 54: Washington (U.S. Govt. Printing Office), 865–877.

Stephenson, A., 1976. A study of rotational remanent magnetization. *Geophys. J. R. Astron. Soc.*, 47:363–373.

\_\_\_\_\_, 1980. Gyromagnetism and the remanence acquired by a rock in an alternating field. *Nature*, 284:48–49.

\_\_\_\_\_, 1981. Gyroremanent magnetization in a weakly anisotropic rock sample. *Phys. Earth Planet. Inter.*, 25:163–166.

Wilson, R. L., and Lomax, R., 1972. Magnetic remanence related to slow rotation of ferromagnetic material in alternating magnetic fields. *Geophys. J. R. Astron. Soc.*, 30:295–303.

Date of initial receipt: 17 August 1989  
 Date of acceptance: 17 January 1990  
 Ms 114B-157

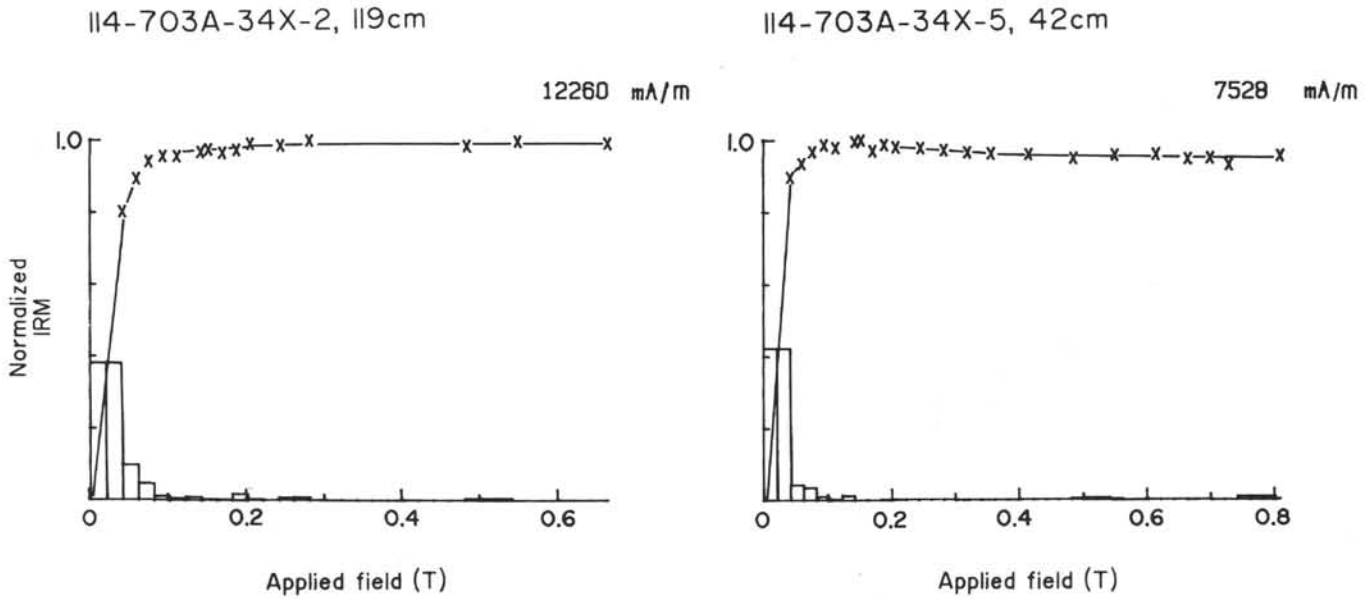


Figure 18. Representative IRM acquisition curves for Hole 703A volcanic breccia samples. The saturation IRM value is also shown.

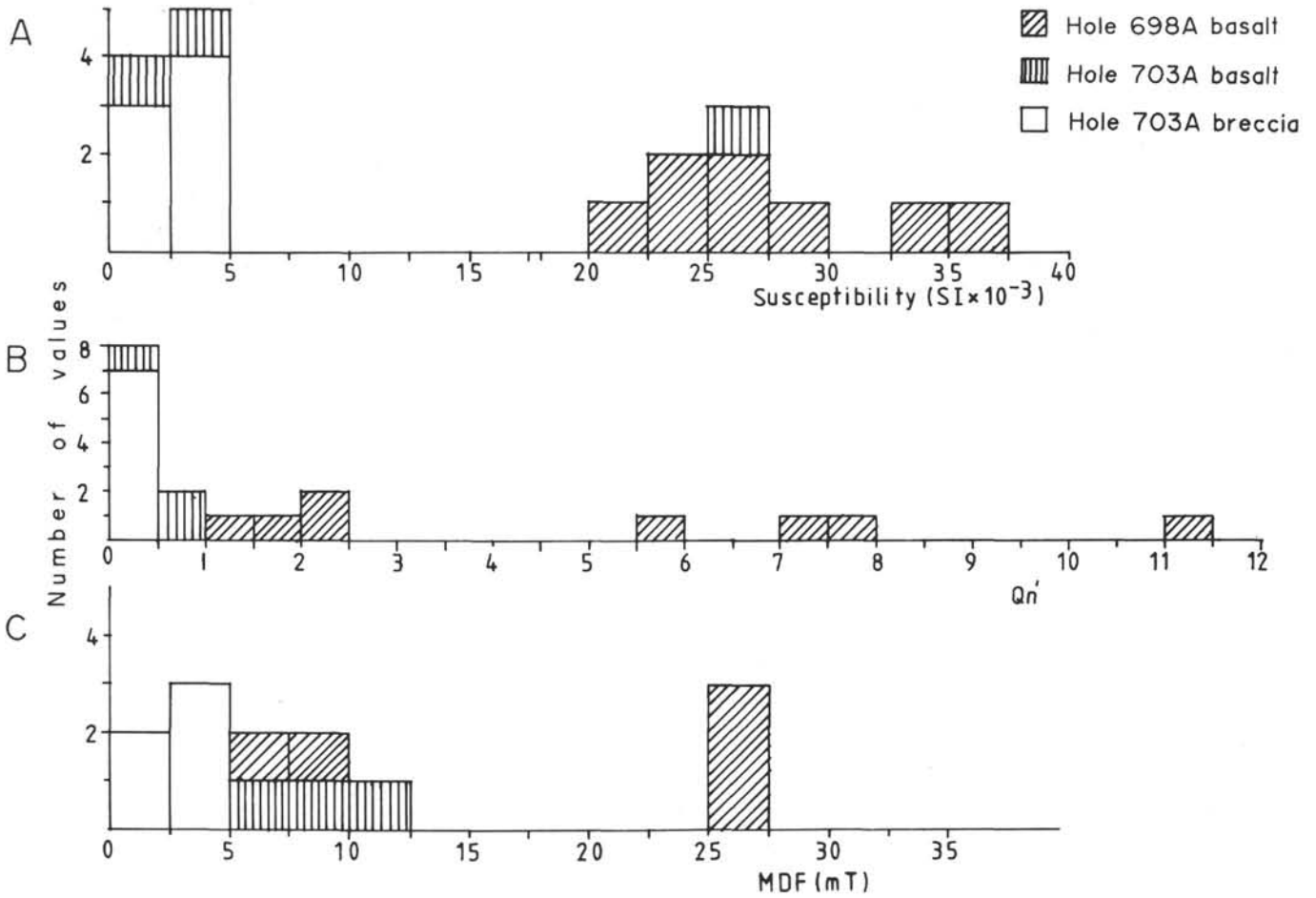


Figure 19. Histograms of (A) volume magnetic susceptibility, (B) Koenigsberger ratio, and (C) MDF values for all samples analyzed.

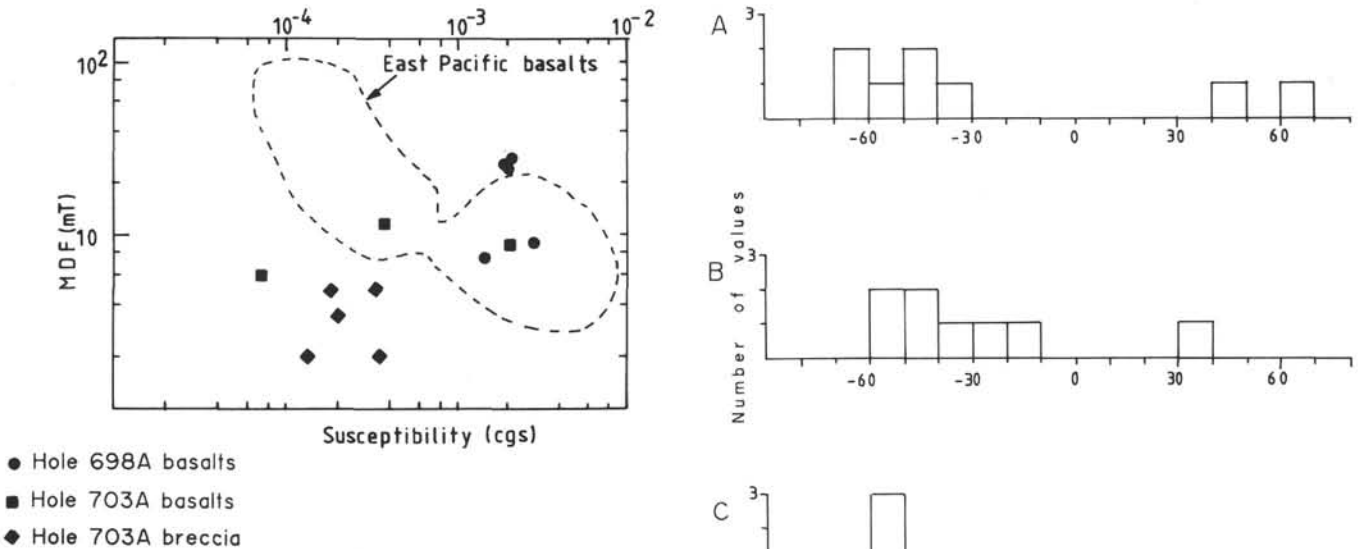


Figure 20. Variation of MDF with volume susceptibility. Values for the Hole 698A basalts and Hole 703A basalts and volcanic breccia are shown, together with the general field occupied by data for submarine basalts from the East Pacific (Petersen and Roggenthen, 1980).

Figure 21. Histograms of inclination values for (A) low, (B) moderate, and (C) high blocking-temperature magnetization components in Hole 698A basalts.